# 2. Experimental Works for Intermediate & Low Pr

## 2.1 Transition to Oscillatory Marangoni Convection in Liquid Bridges of Intermediate Prandtl Number

*Masahiro Kawaji*

*University of Toronto / NASDA*

# TRANSITION TO OSCILLATORY MARANGONI CONVECTION IN LIQUID BRIDGES OF INTERMEDIATE PRANDTL NUMBER

**Masahiro Kawaji[1,3], Fumiaki Otsubo[2], Sanja Simic[1], and Shinichi Yoda[3]**

1. Dept. of Chemical Engineering and Applied Chemistry, University of Toronto, Toronto, Ontario M5S 3E5, Canada
2. A.E.S. Co., Ltd., Tsukuba, Japan
3. National Space Development Agency of Japan, 2-1-1 Sengen, Tsukuba, 305-8505, Japan

Marangoni convection experiments have been conducted with acetone (Pr = 4.3) and methanol (Pr = 6.8) liquid bridges to investigate the flow structures and temperature fields during transition from steady to oscillatory convection in a half floating zone. The disk diameters of 5.0 mm and 10.0 mm were used for both fluids and the liquid bridge height was changed from 1.5 mm to 4.5 mm, covering aspect ratios from 0.3 up to 1.6. Various advanced measurement techniques were employed to yield detailed experimental data useful for both understanding the mechanism responsible for transition as well as verifying linear stability analysis and three-dimensional numerical simulation predictions. In order to reduce the surface evaporation rate, a quartz tube was fitted around the liquid bridge for both fluids. The liquid bridge shape data were obtained for both fluids covering a wide range of volume ratios for each aspect ratio and disk diameter. For acetone, the transition from steady to oscillatory convection was found to occur at disk temperature differences of 1.3 ~ 2.3 K, and liquid temperature fluctuations with amplitudes of 0.02 ~ 0.1 K were detected. For methanol, oscillatory flow appeared at disk temperature differences ranging from 1.6 to 4.3 K. For acetone, the transition was also accompanied by the appearance of an azimuthal component of surface velocity. At the same time, the toroidal vortex started to expand and contract in size, and the radial flow field started to rotate. Although the surface displacement was measured, surface oscillations could not be detected probably because of an insufficient driving force arising from small temperature differences. The critical Marangoni numbers for acetone were found to be higher than the values extrapolated from existing data, due to the effects of evaporation and added heat loss from the liquid surface. On the other hand, the critical Marangoni numbers for methanol showed good agreement with the existing data for a similar Prandtl number.

## 1. INTRODUCTION

A study of Marangoni (or thermocapillary) convection in a cylindrical liquid bridge formed between heated and cooled circular disks is important for understanding the transport processes involved in floating zone crystal growth. The quality of crystals grown may be adversely affected when Marangoni convection undergoes transition from a steady to oscillatory state when the temperature difference, $\Delta T$, between the hot and cold disks exceeds a critical value.

Marangoni convection experiments in half floating zones have been extensively conducted in the past under normal gravity on the ground and microgravity aboard the Space Shuttle and various sounding rockets. It has been experimentally observed that above a certain critical temperature difference, $\Delta T_{cr}$, or the critical Marangoni number, $Ma_{cr}$, which is defined in terms

of $\Delta T_{cr}$, the temperature coefficient of surface tension, $d\sigma/dT$, and liquid bridge's geometrical and thermophysical parameters, Marangoni convection in a half floating zone undergoes a transition from steady to oscillatory convection (Chun and Wuest, 1979; Preisser et al., 1983; Kamotani et al., 1984, among others). For lower values of Marangoni number, a steady flow is observed with a single, axi-symmetric toroidal vortex. If the critical Marangoni number is exceeded, the liquid temperature, flow field and liquid bridge surface have been observed to fluctuate as the flow pattern becomes unsteady and non-axisymmetric (Kamotani et al., 1984; Hirata et al., 1997; Yao et al., 1996).

The basic mechanisms responsible for the onset of oscillatory Marangoni convection, however, are still unclear and the detailed flow structures during the transition need to be fully understood. To this end, a systematic investigation into the key mechanisms is underway at the National Space Development Agency (NASDA) of Japan under the Space Utilization Research Program. This project involves experimental, theoretical and numerical investigations of Marangoni convection instability in half floating zones, covering a wide range of Prandtl numbers, $Pr = \nu / \alpha$, between about $10^{-2}$ and $10^{2}$. The low Prandtl number fluid currently investigated is molten tin ($Pr \approx 0.01$), while the high Prandtl number fluids being studied include silicone oils of different viscosities with Pr typically greater than 16.

From the past experiments mostly using high Pr number fluids, the critical Marangoni number is known to vary with the Prandtl number, disk diameter, volume ratio and aspect ratio (= height / disk radius or diameter) of the liquid bridge. The volume ratio, VR, is defined as the actual liquid volume divided by the volume of the liquid bridge with a shape of a straight cylinder. For each aspect ratio, the instability mode has been determined from experiments and also predicted by linear stability analyses (Kuhlmann and Rath, 1993).

Regarding the oscillation mechanism, Chun and Wuest (1979) postulated that the azimuthally travelling non-axisymmetric disturbance pattern causes the temperature oscillation. On the other hand, Kamotani et al. (1984) suggested that triple coupling among the velocity and temperature fields, and the surface deformation is responsible for the oscillation phenomenon. Strong and weak convection periods would occur alternately at different radial planes and interact in such a way that the entire flow structure becomes non-axisymmetric. The importance of surface deformation for the onset of oscillations was experimentally studied by Yao et al. (1996) for 10 cSt silicone oil. The results indicated that the onset of free surface oscillation occurs earlier than that of temperature oscillations, but the connection between the free surface oscillation and the temperature oscillation was not fully clarified.

Although high Prandtl number fluid experiments have yielded a significant amount of flow and temperature field data in the past, numerical simulations of such experiments encounter considerable difficulties due to the reduction in the thermal boundary layer thickness and its implications for finer grid resolution. On the other hand, although numerical simulations can be more readily performed, experiments using low Prandtl number fluids, such as molten metals and semi-conductors, face considerable challenges in detailed measurements of flow and thermal fields, because the fluids are opaque and susceptible to surface oxidation at high temperatures. Although Hibiya et al. (1999) have successfully used an X-ray to track the motion of tracer particles in a half floating zone of molten silicon, and Onuma et al. (1999) were able to observe surface oscillations at a silicon melt surface using a Michelson-type interferometry, it would require a lot of efforts to yield a sufficient amount of data useful for verification of numerical simulations. Thus, detailed experimental data are needed at an intermediate Prandtl number such that both numerical simulation and detailed measurements are possible.

Previously, Preisser et al. (1983) and Velten et al. (1991) have experimentally studied some aspects of transition to oscillatory Marangoni convection for high temperature melts with intermediate Prandtl numbers, KCl (Pr = 1) and $NaNO_3$ (Pr =7). They measured the critical

temperature difference, $\Delta T_{cr}$, and frequency of temperature oscillations for a disk diameter of 6 mm and various aspect ratios. However, to our knowledge, no other experimental data on Marangoni convection in half floating zones of fluids with intermediate values of Prandtl number between 1 and 10 are available in the literature. More data are needed on flow structures for intermediate Pr fluids that not only enable verification of fully transient, three-dimensional numerical simulations, but also provide further insights into the oscillatory convection phenomena.

To this end, Marngoni convection experiments have been conducted using acetone with Pr = 4.3, and methanol with Pr = 6.8, both of which fall between the intermediate Prandtl numbers of 1 and 7 investigated by Velten et al. (1991). The thermophysical properties of acetone and methanol are summarized in Tables 1.1 and 1.2, respectively.

Table 1.1 Thermophysical Properties of Acetone (Boiling Point = 56.2 °C)

| T (°C) | ρ (kg/m$^3$) | μ (mPa s) | $C_p$ (kJ/kgK) | k (W/mK) | Pr (=ν / α) | $H_{fg}$ (kJ/kg) | σ (mN/m) | Vapor pressure (kPa) |
|---|---|---|---|---|---|---|---|---|
| 0 | 813.2 | 0.398 | 2.102 | 0.165 | 5.1 | 542.1 | 26.3 | 7.59 |
| 20 | 790.3 | 0.325 | 2.156 | 0.160 | 4.4 | 524.1 | 22.9 | 21.9 |
| 27 | 782.4 | 0.301 | 2.214 | 0.159 | 4.2 | | 20.3 | 31.6 |
| 47 | 759.6 | 0.250 | 2.265 | 0.152 | 3.7 | | 17.8 | 70.7 |

Note: $d\sigma/dT$= -0.1262 mN/m/K

Table 1.2 Thermophysical Properties of Methanol (Boiling Point = 64.5 °C)

| T (°C) | ρ (kg/m$^3$) | μ (mPa s) | $C_p$ (kJ/kgK) | K (W/mK) | Pr (=ν / α) | $H_{fg}$ (kJ/kg) | σ (mN/m) | Vapor pressure (kPa) |
|---|---|---|---|---|---|---|---|---|
| 0 | 810.0 | 0.817 | 2.386 | 0.208 | 9.4 | 1231.1 | 24.3 | 3.88 |
| 20 | 794.7 | 0.578 | 2.460 | 0.204 | 6.9 | 1191.1 | 22.6 | 5.92 |
| 27 | 784.9 | 0.533 | 2.537 | 0.202 | 6.7 | 1165.4 | 22.0 | 18.4 |
| 47 | 766.2 | 0.409 | 2.674 | 0.197 | 5.55 | 1133.7 | 20.3 | 48.0 |

Note: $d\sigma/dT$= -0.0846 mN/m/K

The objectives of the present experiments using intermediate Prandtl number fluids were to obtain experimental data useful for both understanding the mechanism of transition from steady to oscillatory Marangoni convection in a half floating zone and verification of linear stability analysis and numerical simulation predictions. To achieve these objectives, many different measurement techniques have been used in this work as described below.

## 2. EXPERIMENTAL APPARATUS

The schematic of the experimental apparatus is shown in Fig. 2.1. The test section consisted of upper and lower disks between which an acetone bridge was formed. Acetone has significantly greater volatility than higher-Prandtl number fluids such as silicone oils, which have been extensively used in previous half-floating zone experiments. To reduce the rates of evaporation and thinning of the acetone bridge with time, a quartz tube was fitted with a gap of 2 ~ 3 mm around the liquid bridge. The upper and lower disks with 5 or 10 mm diameters were

made of brass, copper, sapphire or zinc selenide (ZnSe) as summarized in Table 2.1, and heated or cooled using a combination of Peltier elements connected to DC power supplies, and constant temperature circulation baths.

The lower disk had a small hole drilled through the axis so that acetone could be injected into the gap between the upper and lower disks to form a liquid bridge. A syringe was used to inject the liquid, either manually or using a motorized actuator.

To observe radial flow and temperature patterns in the horizontal cross sections using a PIV technique and an infrared imager (Inframetrics Model 760), respectively, a cylindrical rod made of sapphire (5 mm diameter) or zinc-selenide (5 and 10 mm diameter) was used as the upper disk. The infrared transmitting characteristics of zinc-selenide (65% ~ 70% transmission at wavelengths between 0.8 μm and 14 μm) allowed measurements of a radial temperature profile just below the upper disk within about 0.5 mm using an infrared imager as suggested by Otsubo et al. (1999). On the other hand, the sapphire rod was used for PIV measurements of radial flow patterns since it transmitted blue light from an Argon laser scattered by the tracer particles.

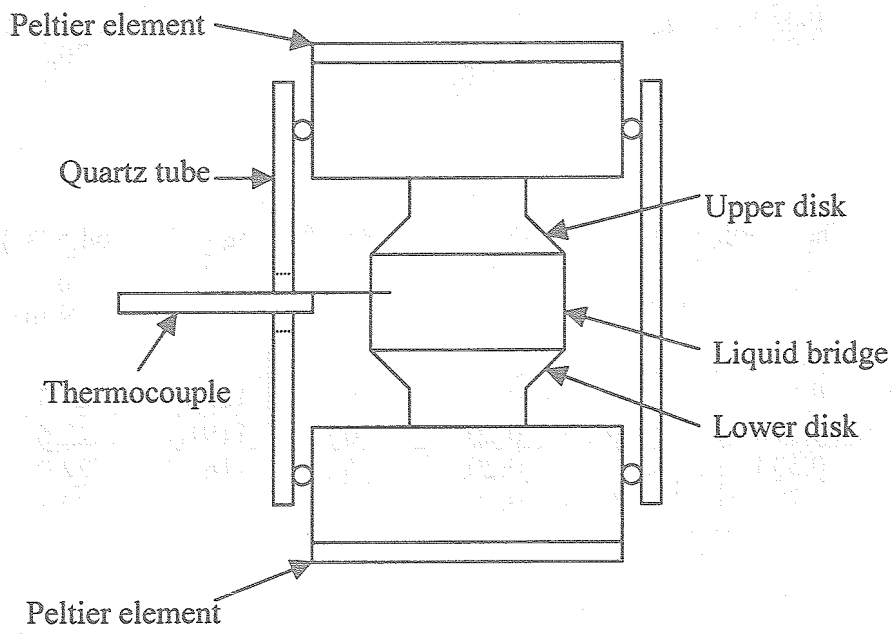


Figure 2.1 Schematic of Marangoni convection experiment apparatus

Table 2.1 Disk materials used

| Diameter (mm) | Lower disk / Upper disk |
|---|---|
| 5.0 | Copper/ZnSe and copper/sapphire |
| 10.0 | Copper/copper and copper/ZnSe |

# 3. INSTRUMENTATION

## 3.1 Disk and Fluid Temperature Measurements

Thermocouples were used to accurately measure the individual disk temperatures, $T_H$ and $T_C$, the disk temperature difference, $\Delta T$, and liquid temperature, $T_f$. In preliminary experiments, the onset of oscillatory Marangoni convection in acetone liquid bridges was found to occur at $\Delta T \approx 2$ K, with the liquid temperature fluctuation amplitudes of the order of 0.1 K. Thus, the thermal data had to be obtained with precisely calibrated thermocouples (T/C's) and recorded by a data acquisition system with little noise.

The disk temperatures were measured using type-T thermocouples with a wire diameter of 75 μm attached to the inside (brass and copper) or outer surface (ZnSe and Sapphire) of upper and lower disks. For $\Delta T$, a pair of type-T thermocouples attached to the disks were connected in series and the cold junctions were enclosed in a thick-walled aluminum box to directly measure the temperature difference.

Liquid temperature fluctuations were measured using a type-E micro-thermocouple with a wire size of 25 μm inserted into the liquid bridge from the side through a hole drilled on the quartz tube wall. The thermocouple junction was positioned just inside the liquid surface between the upper disk and mid-height.

Calibration of all the thermocouples was conducted using a pre-calibrated platinum resistance thermometer sensor (Pt-100) with < 0.03 K error. All the disk and fluid thermocouples were calibrated at 0, 15.0, 20.0 and 25.0°C, while the thermocouple pairs for $\Delta T$ measurement were calibrated at 0,1.0, 2.0, 3.0, 7.0 and10.0°C with $T_H$ kept at 24 ~ 25.5°C. The uncertainty in $\Delta T$ measurement was estimated to be ±0.02°C. The calibration data for $\Delta T$ thermocouple pairs used for 5 mm and 10 mm disks in both acetone and methanol experiments are shown in Figures 3.1 and 3.2, respectively. The thermocouple pair readings for both disk diameters were about 5% higher than the platinum sensor readings.

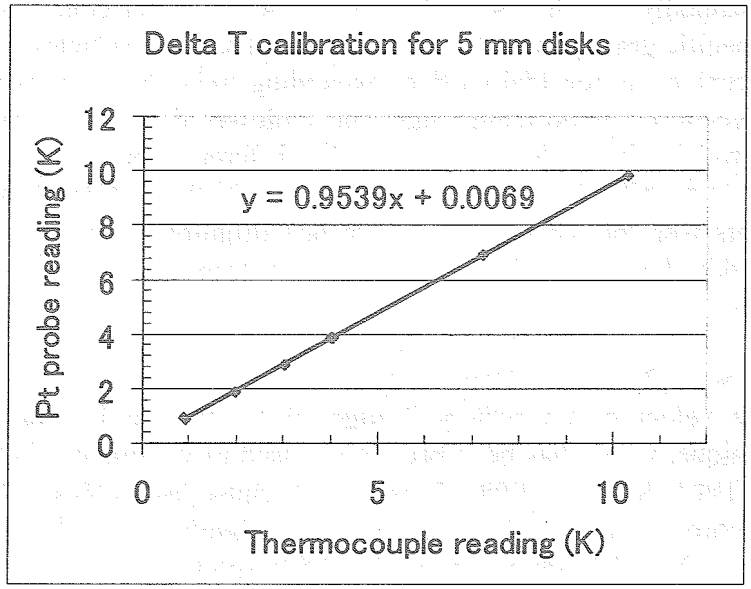


Fig. 3.1 Calibration data for a thermocouple pair measuring disk temperature differences for D = 5.0 mm

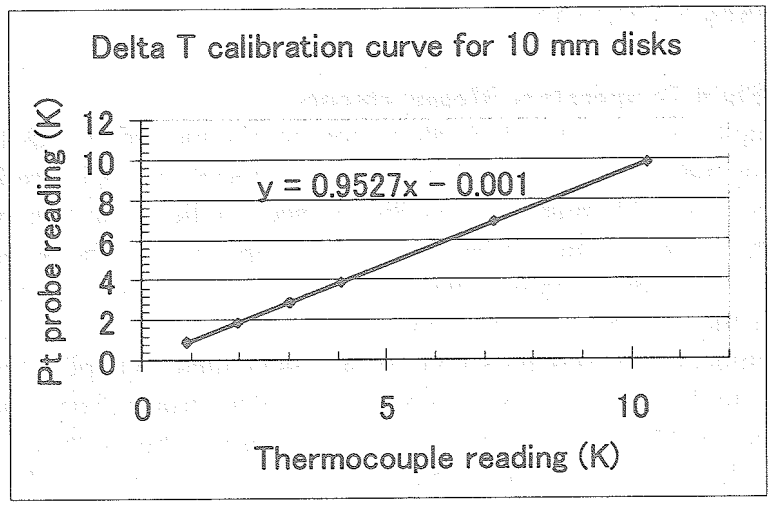


Fig. 3.2 Calibration data for a thermocouple pair measuring disk temperature differences for D = 10.0 mm

To sample and record the temperature data nearly free of noise, a Hewlett-Packard Data Acquisition/Control Unit (Model 3852A) and workstation were used in acetone experiments. The data were sampled using Labview software at a rate of 10 Hz, stored in files and graphically displayed in real-time. With this temperature measurement system, fluid temperature fluctuations of 0.01 ~ 0.02 K amplitude could be clearly identified and recorded. For methanol experiments, a PC-based data acquisition system was used.

### 3.2 Flow Visualization

#### 3.2.1 PIV

The PIV and photochromic dye activation techniques were used to measure the bulk flow pattern and surface velocity in acetone liquid bridges, respectively. For PIV with either a vertical or horizontally oriented laser sheet illumination, silver-coated particles of 8 ~ 12 μm diameter and specific gravity of 1.05 ~ 1.15 were used as seed particles. The vertical light sheet allowed measurements of toroidal vortices expanding and contracting with time at the onset of oscillatory convection. The horizontal light sheet allowed detection of rotational motion in the radial plane as well as the mode of oscillation for different aspect ratios.

In addition, to monitor general flow patterns with back-lighting, Fillite particles with 32 ~ 53 μm diameters were mixed with the liquid and illuminated by a cold light source placed behind the liquid bridge. The Fillite particle motion was monitored with a CCD camera situated at the side of the liquid bridge.

#### 3.2.2 Photochromic Dye Activation Method

The surface velocities on acetone bridges were measured using a photochromic dye activation technique, which has been previously used in various gas-liquid flow experiments (Kawaji et al., 1993; Kawaji, 1998). It uses a UV pulse laser ($N_2$ gas laser, $\lambda$ = 337 nm) to activate photochromic dye (TNSB) molecules dissolved in the working liquid at a concentration of 100 ~ 500 ppm. The acetone-dye solution is transparent, but changes to a purple color upon UV irradiation. The purple liquid acts as a tracer, the motion of which can be monitored by a color video camera to obtain the liquid surface velocity as shown in Fig. 3.3. Although the laser beam penetrated some distance into the liquid, the fastest moving part of the tracer from near the top to the bottom of the liquid bridge can be considered to represent the surface velocity.

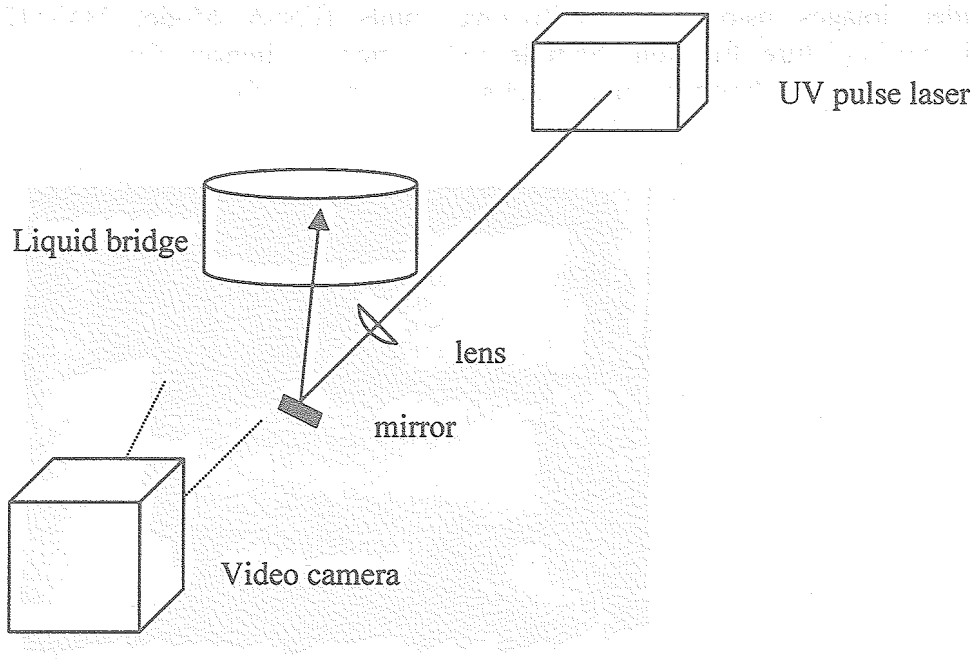


Figure 3.3 Photochromic dye activation set-up for surface velocity measurement

At the onset of oscillatory Marangoni convection, the dye tracer motion changed from a purely one-dimensional (downward) trajectory to a two-dimensional trajectory with an azimuthal displacement as well. Although the same technique has been used previously to measure the velocity of a liquid layer surface in an open boat under Marangoni convection (Tudose and Kawaji, 1999 and 2000), to our knowledge, this work presents the first direct measurement of surface velocity fluctuations at the onset of oscillatory Marangoni convection in a half floating zone.

### 3.3 Surface Oscillation Measurement

Another important feature of this work was an attempt to detect surface oscillations which have been hypothesized to play an important role in the mechanism governing the onset of oscillatory Marangoni convection in a half floating zone at high Prandtl numbers (Kamotani et al., 1984). Recently, Kitagawa et al. (1999) successfully used a Laser Focus Displacement Meter (Keyence Model LT-8100) to measure surface oscillations in 10 cSt silicone oil liquid bridges. Thus, the same instrument with 0.2 μm resolution was first tested with the present experimental apparatus and silicone oil bridges (D = 5 mm) of decreasing viscosity, 2 cSt and 0.65 cSt. The surface oscillations could be detected for 2 cSt silicone oil, however, it became increasingly difficult to detect them for the 0.65 cSt sample.

As explained later, surface oscillations could also be detected for acetone at $\Delta T$ values well above the critical temperature difference, but the amplitude of surface oscillations was too small to be detected at the onset of oscillatory convection.

### 3.4 Simultaneous Recording of Image and Thermal Data

To facilitate data analysis and simultaneous interpretation of the video images and thermal data, CCD and infrared imager signals were combined with the liquid temperature fluctuation and disk temperature difference ($\Delta T$) data on a video monitor and recorded on the same digital video (DV) tape. The thermal data were displayed graphically on a workstation in real-time using Labview and the graphical image was converted to an NTSC signal and combined with

video images using two Multiviewer units (For-A Model MV-112) which had a picture-in-picture function. Sample video monitor images from acetone and methanol experiments are shown in Figures 3.4 and 3.5, respectively.


Figure 3.4 Simultaneous recording of video and thermal data in acetone experiments

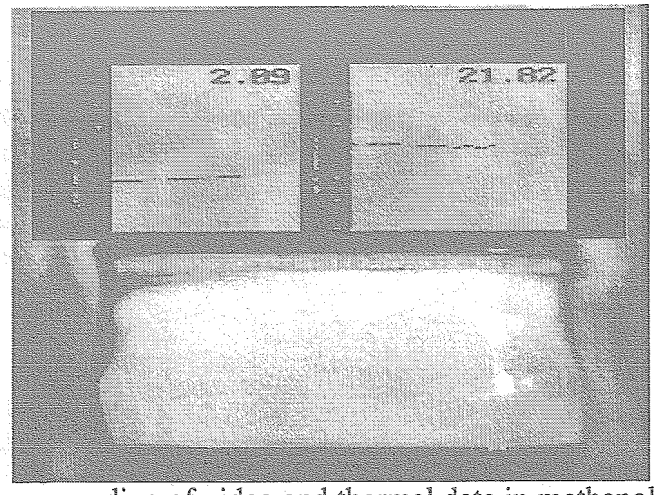


Figure 3.5 Simultaneous recording of video and thermal data in methanol experiments

## 4. EXPERIMENTAL PROCEDURE AND CONDITIONS

The experimental parameters investigated in the present work were the disk diameter, D (=2R), liquid bridge height, H, or aspect ratio, AR (=2H / D or H / Radius), and the volume ratio, VR, which is the ratio of the actual liquid bridge volume to the volume of a right cylinder of diameter, D, and height, H. For each disk diameter, the liquid bridge height (or aspect ratio) was fixed at a specified value as shown in Table 4.1, and $\Delta T$ was varied slowly by changing the voltage supplied to the Peltier element attached to the lower disk, while the upper disk temperature was kept nearly constant. Similar experimental parameter ranges were covered and the same procedure was followed in methanol experiments, however, PIV, photochromic dye activation, surface displacement and IR imager measurements are either still underway or not yet performed at the time of preparation of this report.

Table 4.1 Experimental Conditions for Acetone Experiments

| Diameter, 2R (mm) | Height, H (mm) | Aspect ratio (H/R) | Volume Ratio[1] | Instrumentation Used[2] |
|---|---|---|---|---|
| 5.0 | 1.5 ~ 4.0 | 0.6 ~ 1.6 | 0.81 ~ 1.08 | PD, IR |
| 5.0 | 2.7 ~ 4.0 | 1.08 ~ 1.6 | < 1.0 ~ > 1.0 | PIV |
| 10.0 | 1.5 ~ 4.0 | 0.3 ~ 0.8 | 0.84 ~ 1.06 | PD, IR |
| 10.0 | 2.5 ~ 3.5 | 0.5 ~ 0.7 | < 1.0 ~ >1.0 | PIV |
| 10.0 | 2.7, 3.5 | 0.54, 0.7 | < 1.0 ~ >1.0 | LFDM |

Notes:

PD: photochromic dye activation method for surface velocity measurement;
PIV: particle image velocimetry for flow pattern measurement;
IR: infrared imager for cross-sectional temperature distribution measurement;
LFDM: Laser Focus Displacement Sensor

Due to evaporation from the liquid bridge surface, the volume ratio for both liquid bridges decreased slowly and continuously from over 100% to about 80 ~ 90%. Table 4.1 also presents the ranges of parameters covered in acetone experiments including the different types of instrumentation used.

### 4.1 Effects of Impurities in Acetone and Surface Contamination

In order to minimize the effect of impurities contained in the working fluid, acetone of 99.5% and 99.9+% purity were tested both with and without zeolite treatment to reduce the residual water content. The preliminary tests indicated, however, no significant effects of purity and residual water content on the critical $\Delta T$ values measured. Thus, in the present work, acetone of 99.9+% purity and methanol of 99.99% purity both from Aldrich and without any zeolite treatment were used in all the experiments. The temperature-dependent surface tension coefficient was measured with and without a photochromic dye (0.05% concentration) and tracer particles. The surface tension measurements at different temperatures using a Kyowa surface-tensiometer (Model CBVP-Z) and a plate pulling method yielded no significant differences (< 2%) between pure acetone and the working solutions as shown in Figure 4.1.

Although the liquid bridge was surrounded by a quartz tube and not directly exposed to the ambient atmosphere except through the small holes provided for fluid thermocouple insertion, contamination of the acetone bridge surface was suspected to have occurred when the convection speed was noticeably reduced or the critical $\Delta T$ was unusually large. To avoid obtaining data with a contaminated liquid surface, fresh liquid was occasionally injected to overflow from the lower disk and renew the liquid bridge surface.

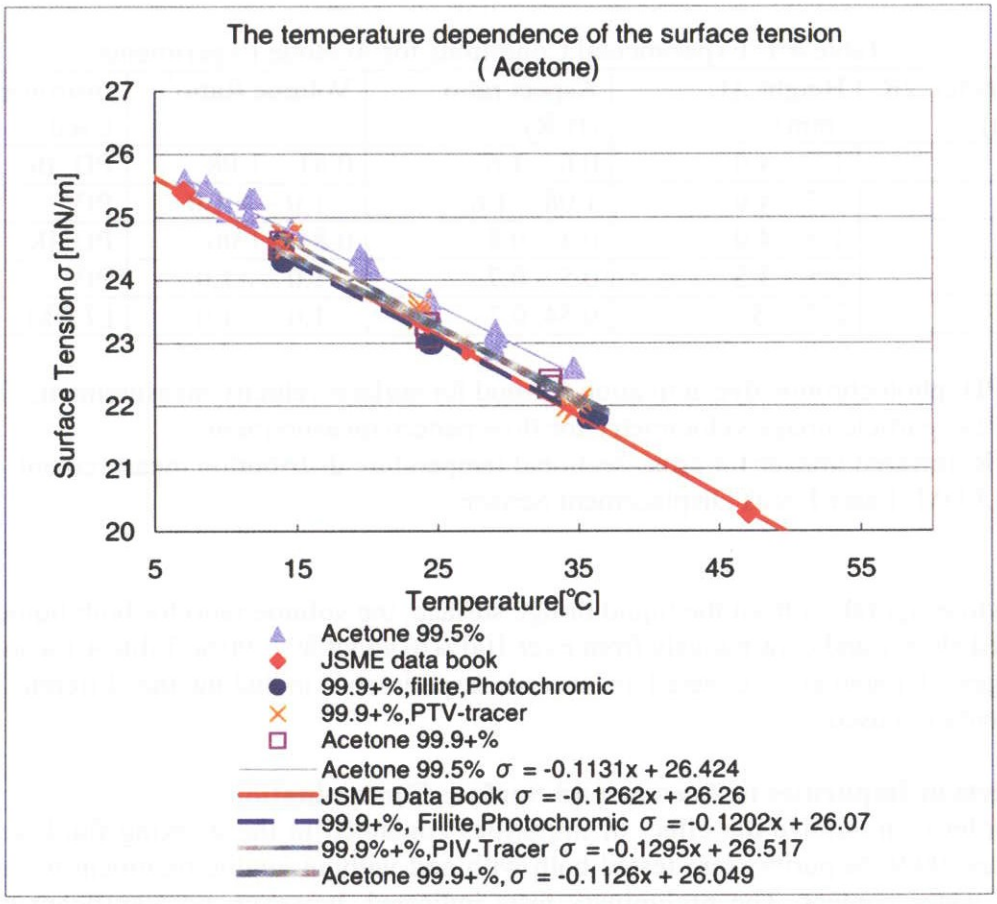


Figure 4.1 Variation of surface tension with temperature for acetone

# 5. DATA ANALYSIS

## 5.1 Bridge Shapes and Evaporation Rates

A typical video image of the acetone bridge for a 10 mm disk diameter and 2.8 mm bridge height is shown in Fig. 5.1. From similar images, acetone and methanol bridge shape data could be easily obtained by capturing the video images and digitizing the shapes using an image analysis program (WINROOF for acetone and MOCHA for methanol) on a PC. Due to the evaporation effect, the volume ratio for both fluids decreased with time. For example, acetone bridge's volume ratio varied from 100 ~ 108% to 85 ~ 95% over a period of 74 ~ 610 seconds. By using the volume ratios obtained at the beginning (VR > 100%) and at the end (VR < 100%) and the time elapsed, the average evaporation rate could be quantified in terms of the volume reduction rate per unit time. As shown in Table 5.1 and 5.2, the evaporation rate decreased strongly with the liquid bridge diameter for both fluids. This is reasonable since the exposed surface area increases linearly with the diameter for a given height, but the liquid bridge volume increases as the square of the diameter. The methanol had a smaller evaporation rate, approximately ¼ ~ 1/5 of acetone.

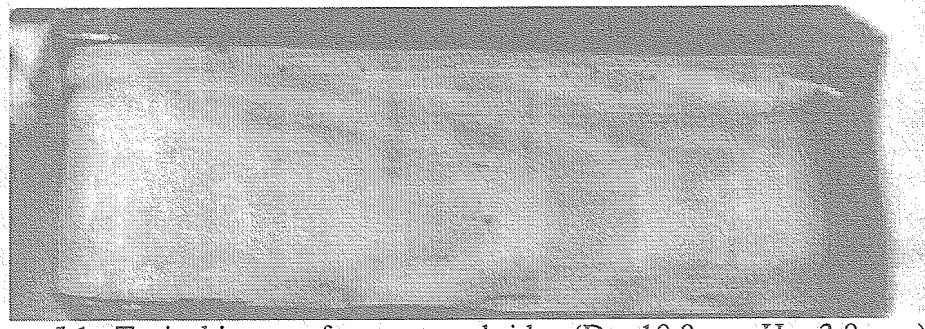

Figure 5.1 Typical image of an acetone bridge (D = 10.0mm, H = 3.0 mm)

Table 5.1 Volume Reduction Rates for Acetone Bridge

| Diameter (mm) | Volume Reduction Rate (%Vol./sec) |
|---|---|
| 5.0 | 0.12 ~ 0.19 |
| 10.0 | 0.03 ~ 0.06 |

Table 5.2 Volume Reduction Rates for Methanol Bridge

| Diameter (mm) | Volume Reduction Rate (%Vol./sec) |
|---|---|
| 5.0 | ~0.05 |
| 10.0 | ~0.01 |

### 5.2 Determination of the Onset of Oscillatory Marangoni Convection

In the experiment, the disk temperature difference, $\Delta T$, was varied to either increase or decrease past the critical value while the volume ratio of the liquid bridge was allowed to slowly decrease from > 100% to < 100% due to evaporation. For each disk diameter and aspect ratio, fluid and disk temperature measurements were made several times to check the reproducibility of the critical temperature difference data at the onset of oscillatory Marangoni convection.

At the onset of oscillatory convection, the following phenomena were observed to occur. Each of these phenomena will be described in more detail in the following sections.

- Periodic fluid temperature fluctuations
- Surface velocity fluctuations with an appearance of azimuthal component
- Vortex expansion and contraction in PIV images
- Variations of radial temperature and flow patterns in cross-sectional views of IR image and tracer particle motion

On the other hand, as mentioned previously, surface oscillations were detectable for acetone only at temperature differences significantly greater than the critical value, $\Delta T >> \Delta T_{cr}$ for D = 5 mm and 10 mm.

### 5.2.1 Liquid Temperature Fluctuations and Detection of Oscillatory Convection

At the onset of oscillatory convection in an acetone bridge, the fluid temperature started to fluctuate periodically with a frequency of about 0.3 ~ 0.7 Hz and an amplitude of 0.02 ~ 0.1 K. Sample acetone data for D = 10 mm and H = 3.0 mm, presented in Fig. 5.2 show a sudden increase in the liquid temperature fluctuation with very small amplitudes (0.01 ~ 0.02 K). The liquid temperature fluctuations were periodic and could be clearly distinguished from the background noise which existed in steady convection. In some cases, the temperature fluctuations were irregular but large enough in amplitude (~ 0.1 K) as shown in Fig. 5.3. Similar appearances of a periodic temperature fluctuation with an increasing amplitude were also observed in methanol experiments as shown in Fig. 5.4. Other plots of liquid temperature fluctuations and disk temperature difference for all acetone and methanol runs are also available but not shown.

The amplitude and periodicity of the fluid temperature fluctuations are likely to vary with the fluid thermocouple location inside the liquid bridge with respect to the free surface and the upper and lower disks. Because the liquid surface receded with time due to evaporation, the T/C junction was always positioned slightly inside the free surface. Also, because the fluid thermocouple had to be inserted through a small hole in the glass tube surrounding the liquid bridge, it was difficult to always position the T/C junction at the same position relative to the upper disk in runs with different bridge heights.

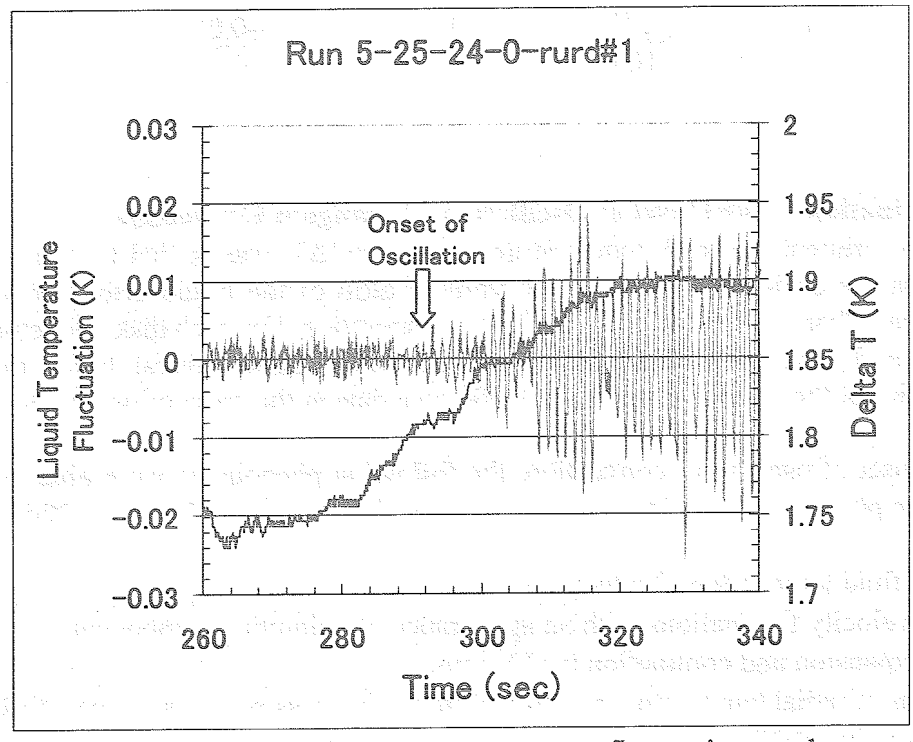


Figure 5.2 Variation of acetone temperature fluctuations at the onset of oscillatory convection (D = 5.0 mm, H = 2.5 mm)

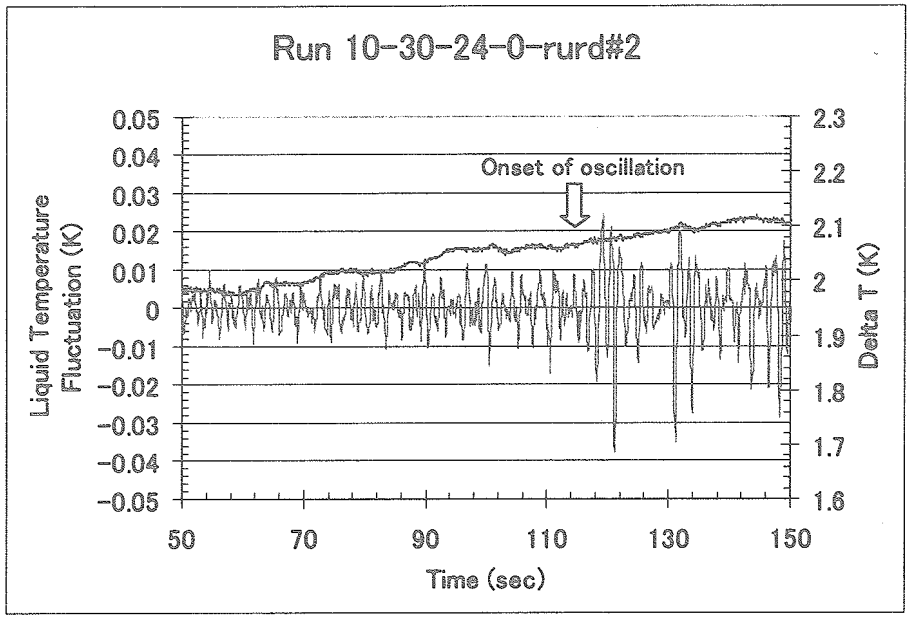


Figure 5.3 Irregular acetone temperature fluctuations after the onset of oscillatory convection (D = 10 mm, H = 3.0 mm)

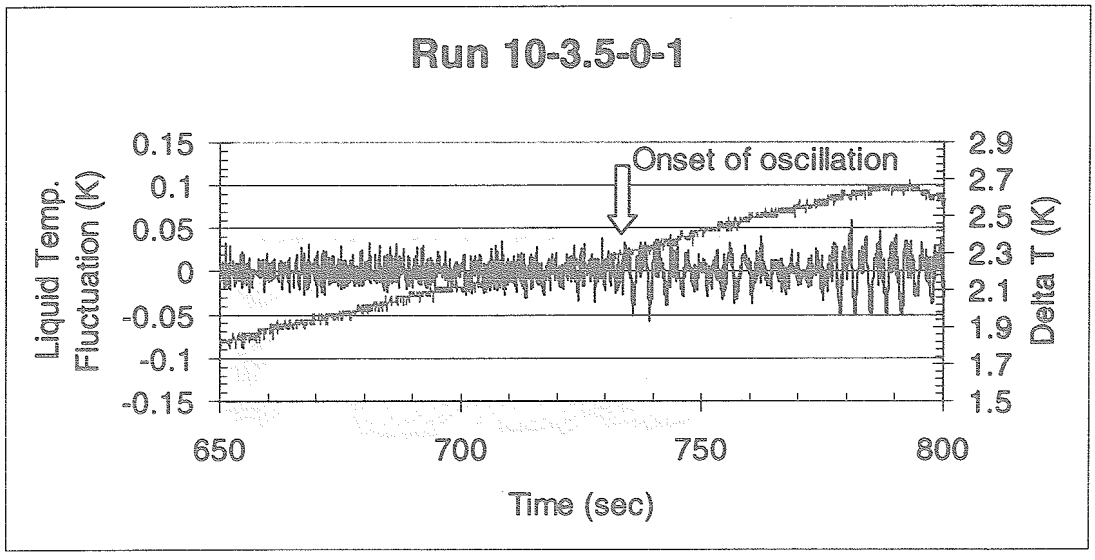


Figure 5.4 Onset of periodic temperature oscillation in methanol bridge (D = 10 mm, H = 2.5 mm)

### 5.2.2 Other Indications of the Onset of Oscillatory convection

For acetone, the flow visualization and other types of measurements revealed additional changes taking place at the onset of oscillatory flow. For methanol, the measurements are still underway, but similar changes are also expected. Each of these phenomena occurring at the onset of oscillatory flow will be discussed in detail below.

**Surface Velocity Fluctuations**

As a pulse of the UV laser beam was shot on the liquid surface just below the upper disk, a

purple-colored dye trace formed instantaneously and moved downward. Although the UV beam penetrated into the liquid and created a short line trace normal to the free surface, the trace appeared initially as a single spot when viewed from outside parallel to the beam direction as illustrated in Fig. 5.5.

As the surface liquid moved downward due to the surface tension gradient, so did the dye trace. The trace movement observed can be considered to represent the surface velocity because every trace always reached close to the lower disk unlike the Fillite tracer particles, many of which were seen to move much shorter vertical distances because they were moving inside the free surface, and not directly on the free surface.

In steady flow at $\Delta T < \Delta T_{cr}$, dye traces formed near the upper disk always traveled to the same azimuthal location near the lower disk. In many cases, the trace trajectory was not perfectly vertical but inclined somewhat, indicating a small but constant azimuthal component of velocity.

At the onset of oscillatory flow, the dye trace trajectory started to fluctuate in the azimuthal direction, towards the left and right as illustrated in Fig. 5.6. This surface velocity fluctuation was observed to occur nearly simultaneously with the appearance of liquid temperature fluctuations described previously. The azimuthal component of surface velocity changed its direction and magnitude continuously. This is, to our knowledge, the first time that the surface velocity and its fluctuations have been directly measured in a half floating zone.

The Fillite particle motion also changed from purely up-down motion to that with left-right motion superimposed on the vertical motion, tracing approximately a figure of eight geometry. Furthermore, with a sufficiently large value of $\Delta T$, the tracer particle motion showed an azimuthally travelling wave. The vertical amplitude of the tracer particle motion at a given azimuthal position oscillated in time, and this amplitude variation around the circumference showed a sinusoidal pattern at a given instant of time. These tracer particle and temperature oscillation data represent the propagation of a hydrothermal wave in the azimuthal direction.

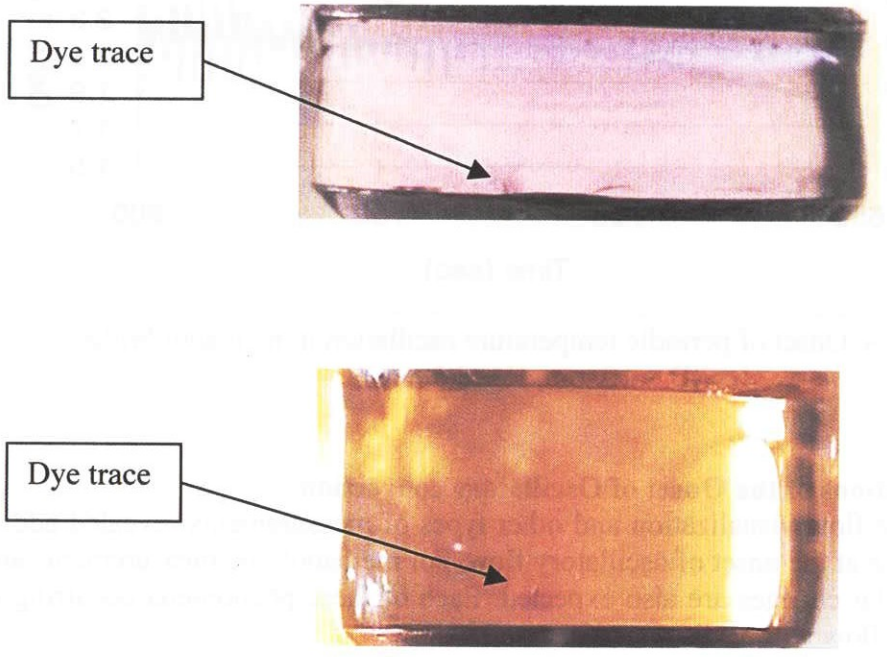


Figure 5.5 Images of a photochromic dye trace moving on the acetone bridge surface

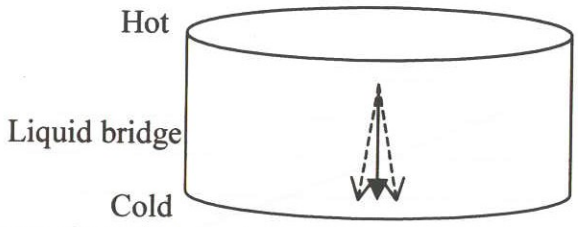

Figure 5.6 Trajectory of photochromic dye traces at the onset of oscillatory convection

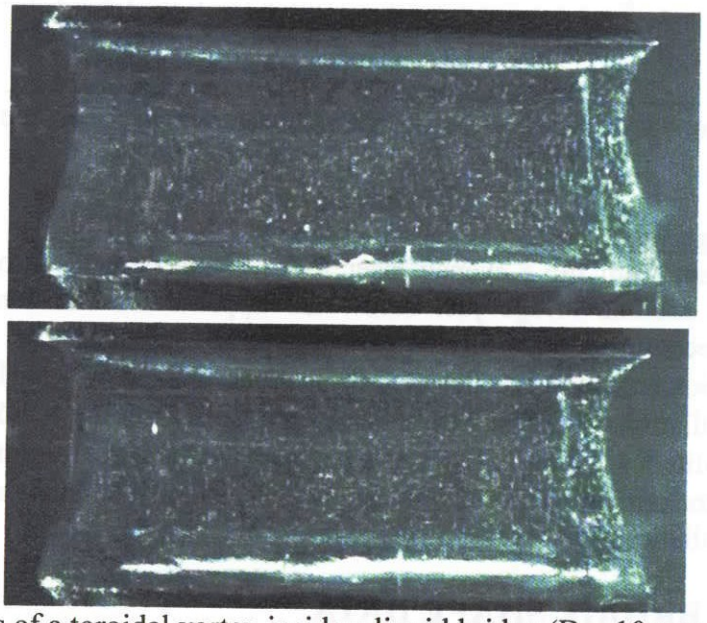
Figure 5.7 PIV images of a toroidal vortex inside a liquid bridge (D = 10 mm, H = 3.5 mm)

**Vortex Expansion and Contraction**

In PIV images of flow patterns in the vertical cross section, a pair of vortices appeared near the liquid bridge surface as shown in Fig. 5.7. At the onset of oscillatory flow, these vortices started to expand and contract at the same frequency as the temperature fluctuations, as previously reported by Chun and Wuest (1979).

**Temporal Variations of Radial Temperature and Flow Patterns**

Rotational oscillations were clearly observed in radial temperature distributions obtained by the IR imager at $\Delta T >> \Delta T_{cr}$, but were difficult to identify at $\Delta T \approx \Delta T_{cr}$. This is most likely due to the small magnitudes of temperature variations below the upper disk induced by small critical temperature differences, $\Delta T_{cr}$, in the order of 1.6 ~ 2.3 K for acetone. On the other hand, PIV images of the radial flow patterns in the horizontal mid-plane clearly showed fluctuations and in many cases, rotational motion at the onset of oscillatory flow. At $\Delta T >> \Delta T_{cr}$, these radial flow pattern oscillations clearly showed a specific instability mode depending on the aspect ratio.

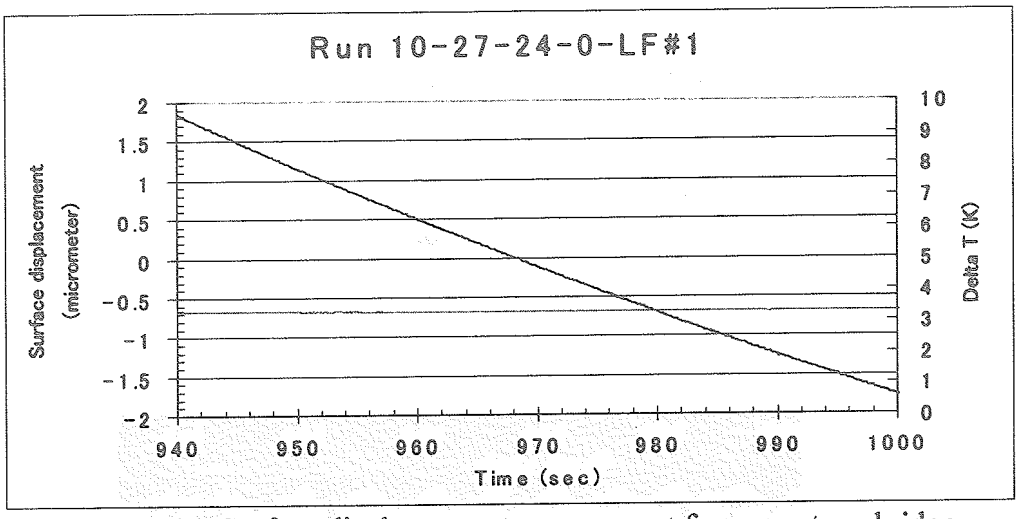


Figure 5.8 Surface displacement measurement for an acetone bridge

**Surface Oscillations**

A laser beam from the Keyence laser focus displacement sensor was focussed on the surface of the acetone bridge just below the upper disk. The sensor signal indicated a continuously receding surface due to evaporation as shown in Fig. 5.8. Unfortunately, the surface oscillations could not be detected for acetone at $\Delta T \approx \Delta T_{cr}$ for D = 5 and 10 mm. Since the surface oscillations could be barely detected even at large $\Delta T >> \Delta T_{cr}$ for acetone, surface oscillation amplitudes at $\Delta T = \Delta T_{cr}$ must have been less than the minimum sensor resolution of 0.2 μm or that the critical $\Delta T$ of ~ 2.0 K may not be sufficient to create a sufficient driving force for surface oscillations to occur.

## 6. LIQUID BRIDGE SHAPE DATA

Typical images and shape data for acetone and methanol liquid bridges are shown in Figures 6.1 through 6.7. From the bridge shapes, the volume ratios could be readily obtained by numerically integrating the average radius between the top and bottom of the bridge. The volume ratio (VR) data are used in the next section to select the critical temperature difference data for VR~1.0 in order to compare with the existing data for Pr = 1 ~ 7 reported by Velten et al. (1991).

Height = 1.5mm, Aspect Ratio = 0.6

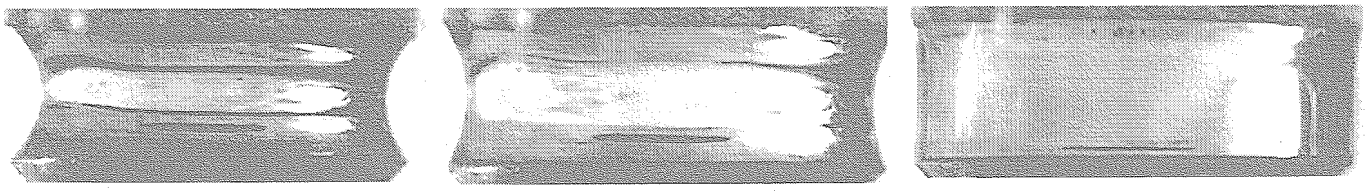

VR=0.83 VR=0.90 VR=0.95

Height =2.5mm, Aspect Ratio =1.0

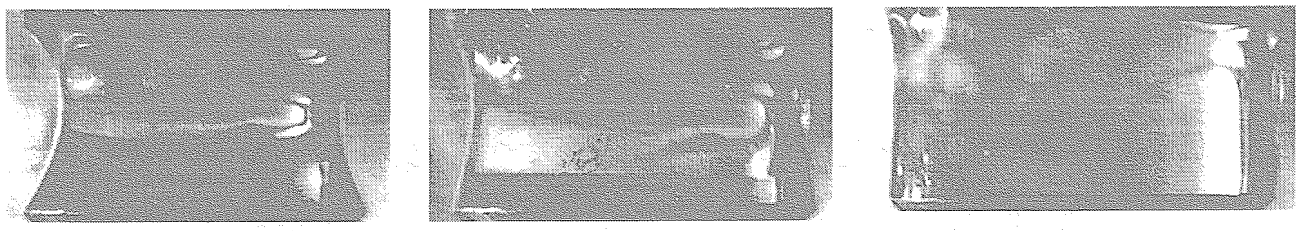

VR=0.78 VR=0.91 VR=0.98

Height = 4.0mm, Aspect ratio = 1.6

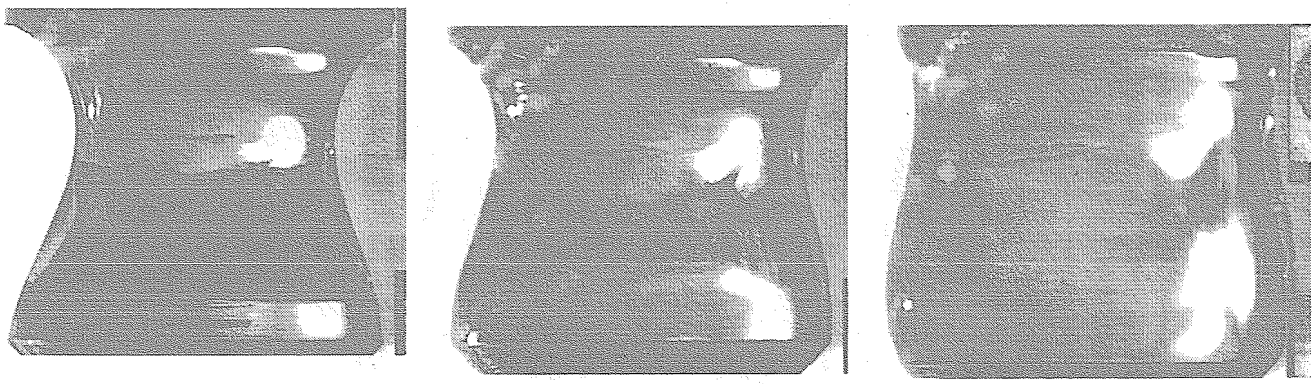

VR=0.66 VR=0.74 VR=1.06

Figure 6.1 Images of an acetone bridge for D = 5.0 mm and various aspect and volume ratios

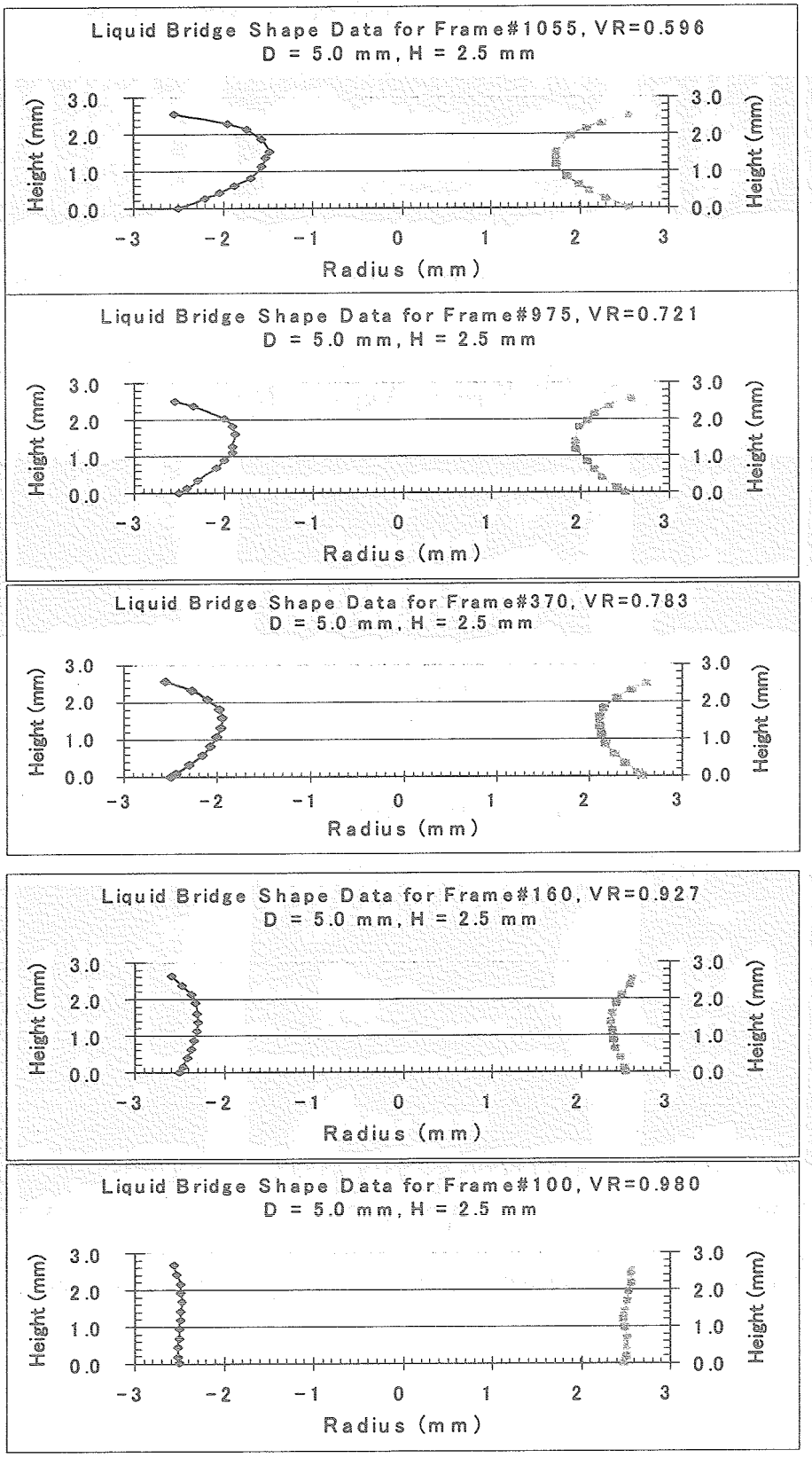


Figure 6.2 Acetone bridge shape data for D = 5.0 mm, H = 2.5 mm and various volume ratios

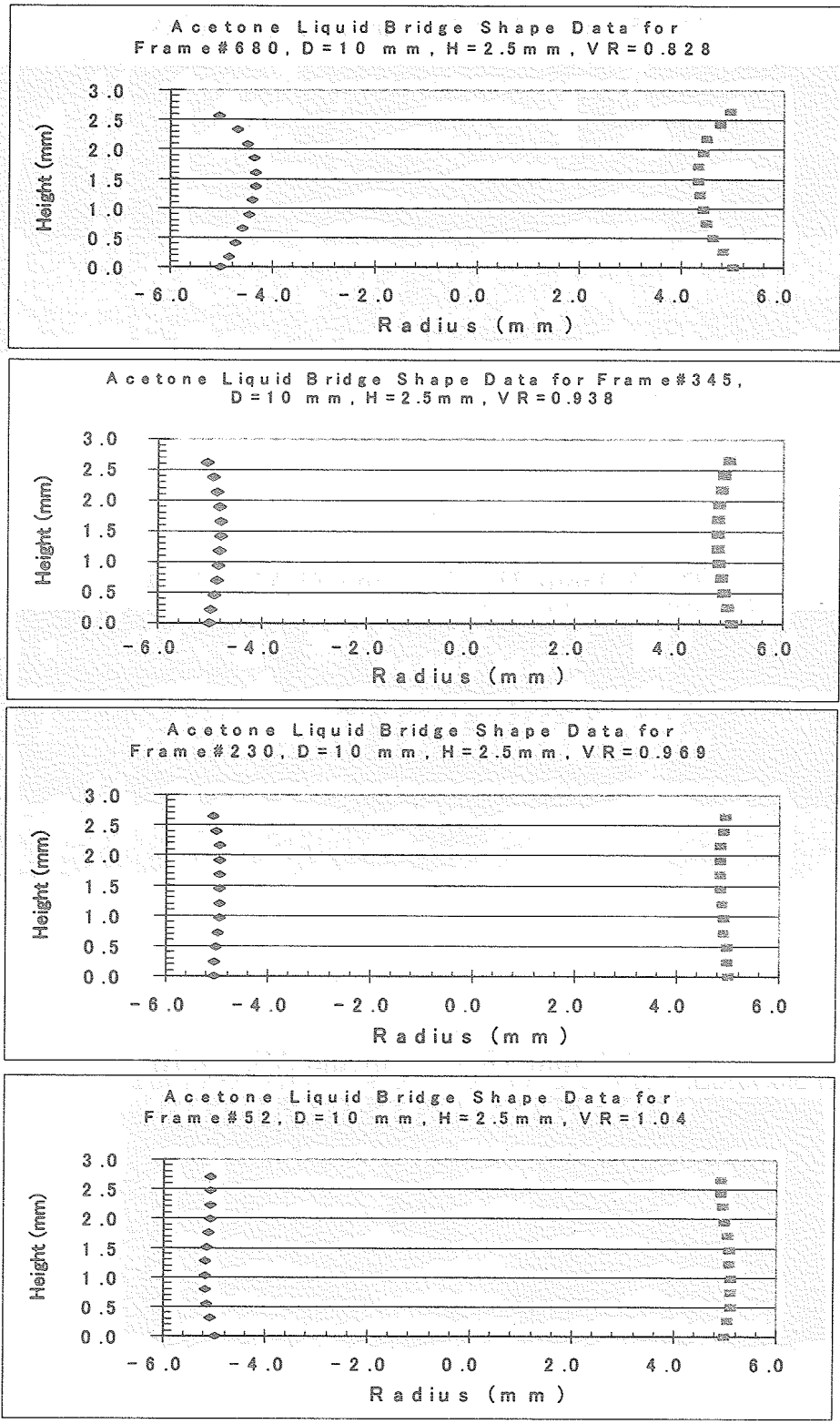


Figure 6.3 Acetone bridge shape data for D = 10.0 mm, H= 2.5mm, and various volume ratios

D = 5.0 mm, H = 1.7 mm and AR = 0.68

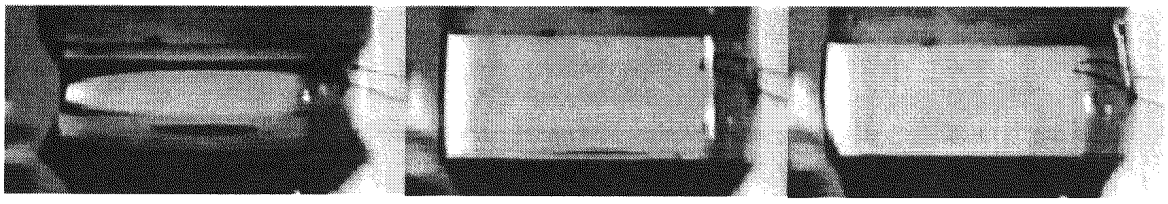

D = 5.0 mm, H = 2.6 mm and AR = 1.04

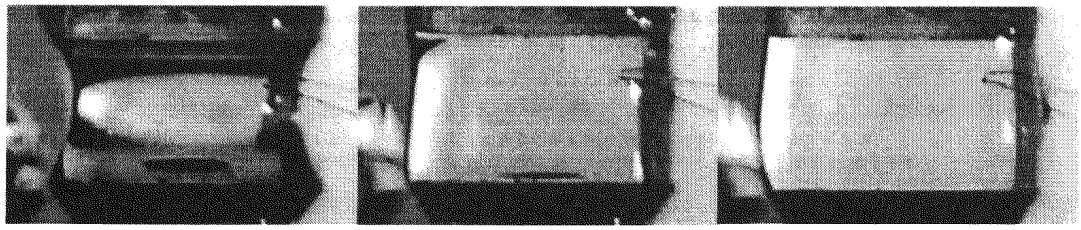

D = 5.0 mm, H=4.4 mm and AR = 1.76

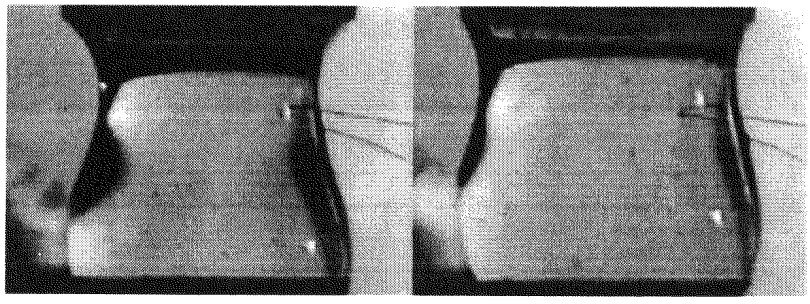

Figure 6.4 Images of a methanol bridge for D = 5.0 mm and various aspect and volume ratios

D = 10 mm, H = 2.8 mm and AR = 0.56

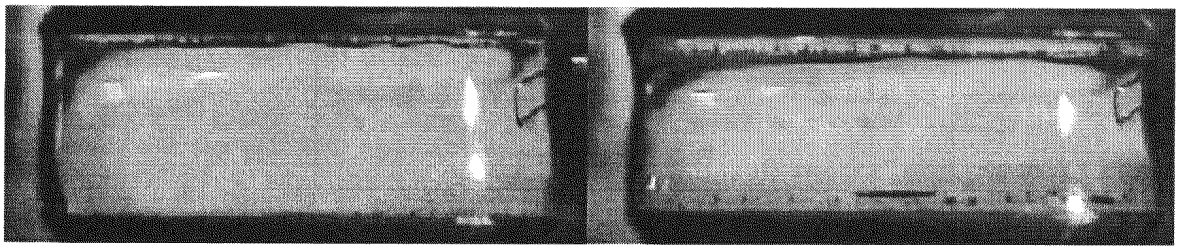

D = 10 mm, H = 4.3 mm and AR = 0.86

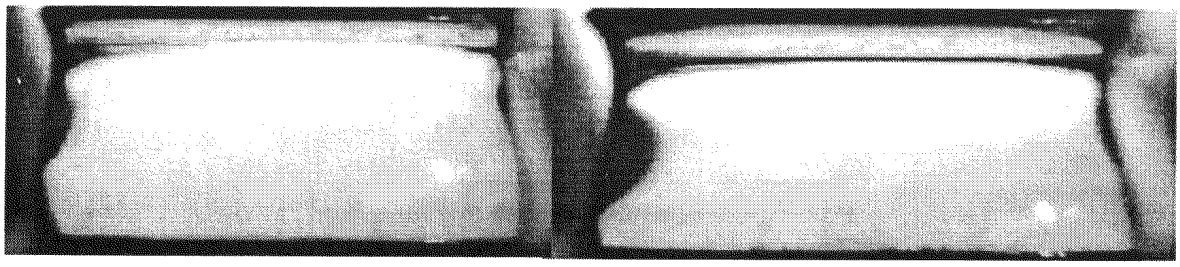

Figure 6.5 Images of a methanol bridge for D = 10.0 mm and various aspect and volume ratios

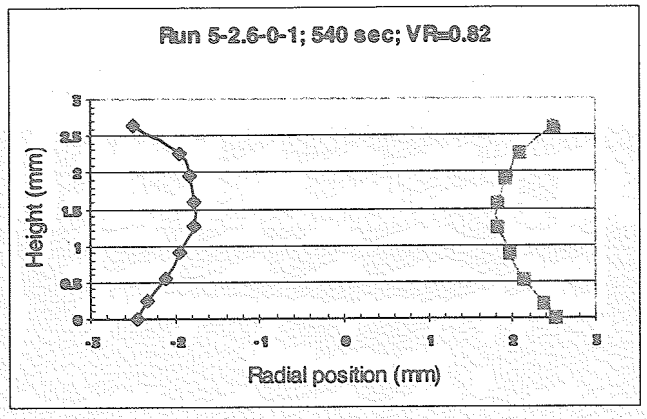


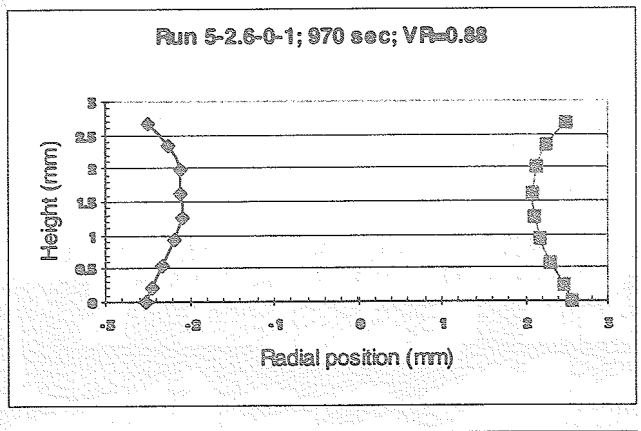


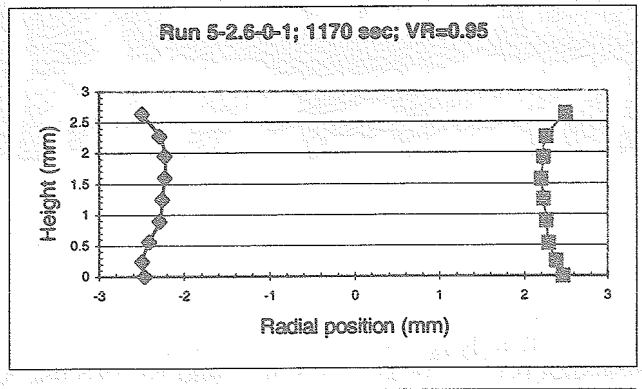


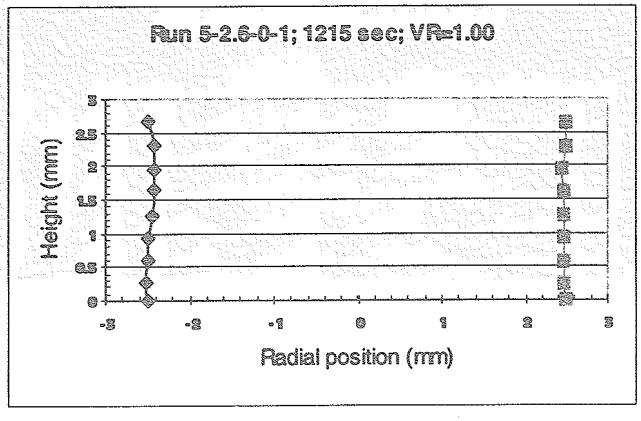


Figure 6.6 Methanol bridge shape data for D = 5.0 mm, H = 2.7 mm, AR =1.08

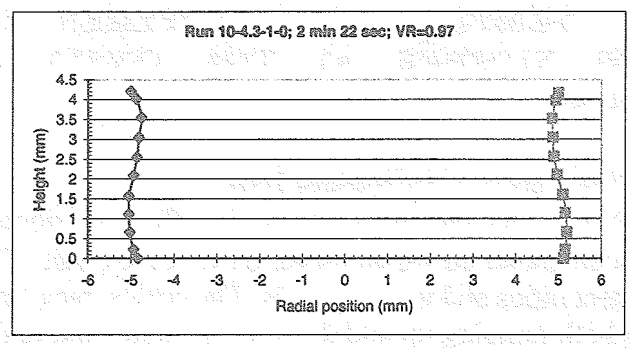


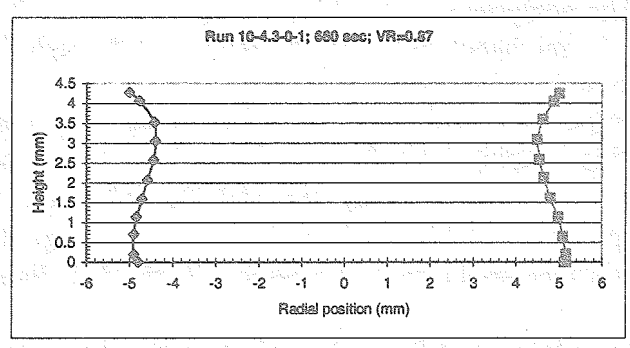


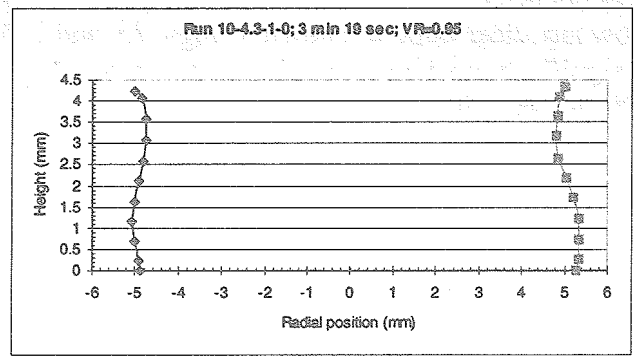


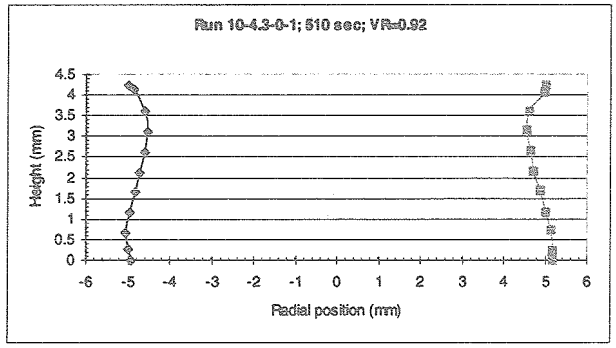


Figure 6.7 Methanol bridge shape data for D = 10.0 mm, H = 4.3 mm, AR =0.86

# 7. CRITICAL TEMPERATURE DIFFERENCE AND CRITICAL MRANGONI NUMBER AT THE ONSET OF OSCILLATORY CONVECTION

## 7.1 Critical Disk Temperature Difference Data

Liquid temperature fluctuations detected by fluid thermocouples were examined to determine the critical temperature difference, $\Delta T_{cr}$, at the onset of oscillatory flow for various disk diameters, aspect ratios and volume ratios. The critical temperature data were obtained for both fluids during both ramping up and down of the temperature difference as shown in Figs. 7.1 through 7.4. The analyses showed $\Delta T_{cr}$ to range from ~1.6 K to ~2.3 K for acetone, and from ~1.6 to 4.3 K for methanol, as shown in Figures 7.5 through 7.8 as a function of the aspect ratio for two different disk diameters.

The critical temperature differences for ramping up were generally slightly higher than those obtained during ramping down for both fluids. This is reasonable since it takes some time for the oscillatory flow field to decay and stabilize when $\Delta T$ falls below $\Delta T_{cr}$. While a relatively weak dependence of $\Delta T_{cr}$ on the disk diameter and aspect ratio was found for acetone, the values of $\Delta T_{cr}$ for methanol clearly increased with the disk diameter and decreased with the aspect ratio.

Concerning the dependence of $\Delta T_{cr}$ on the volume ratio, the acetone results for D = 5mm and 10 mm did not show any clear trend as shown in Figs. 7.9 and 7.10. The data examined so far have indicated no significant peaking at a volume ratio near 100% as numerically predicted by Chen and Hu (1998) for Pr = 10.

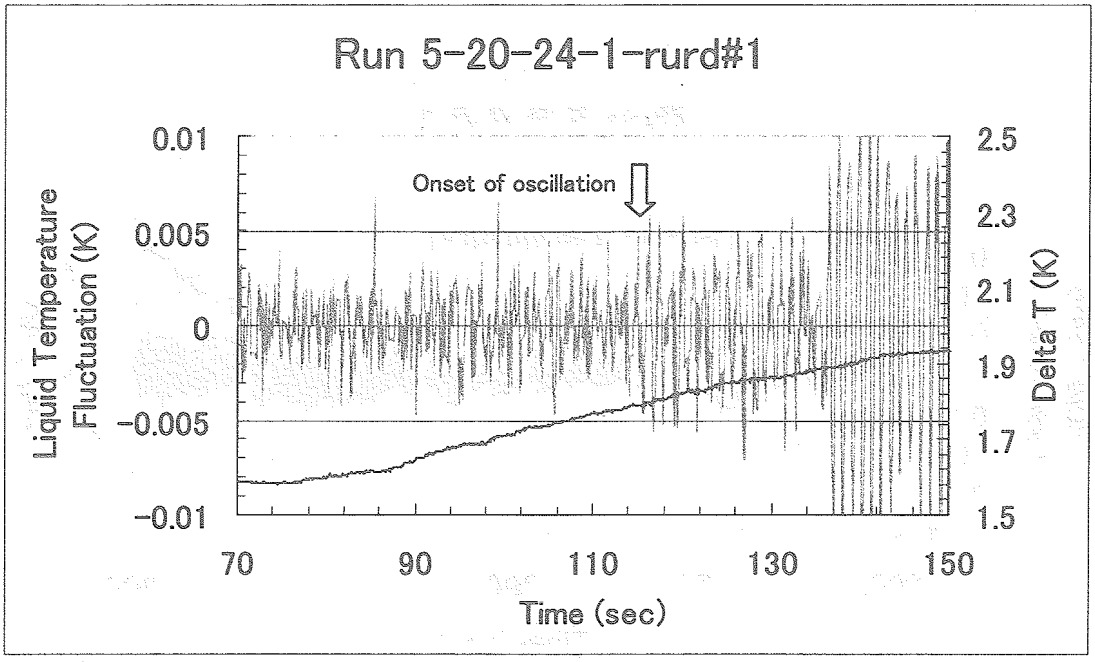


Figure 7.1 Acetone bridge temperature and disk temperature variations at the onset of oscillatory convection for D = 5.0 mm, H = 2.0 mm, AR = 0.80

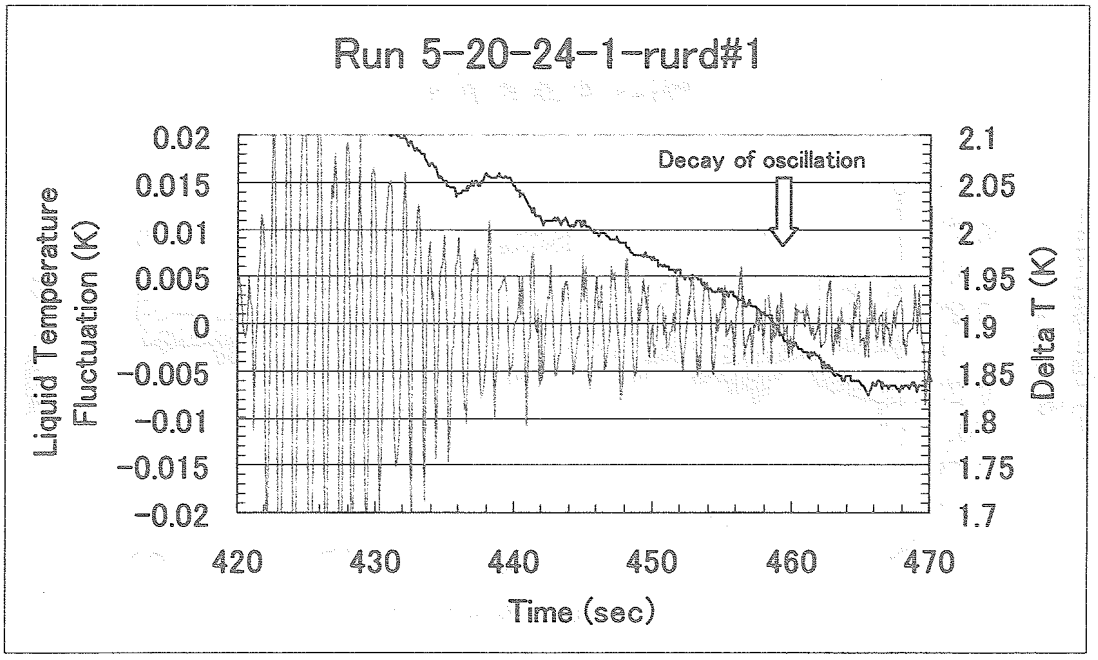


Figure 7.2 Acetone bridge temperature and disk temperature variation at the onset of oscillatory convection for D = 10.0 mm, H = 2.0 mm, AR = 0.80

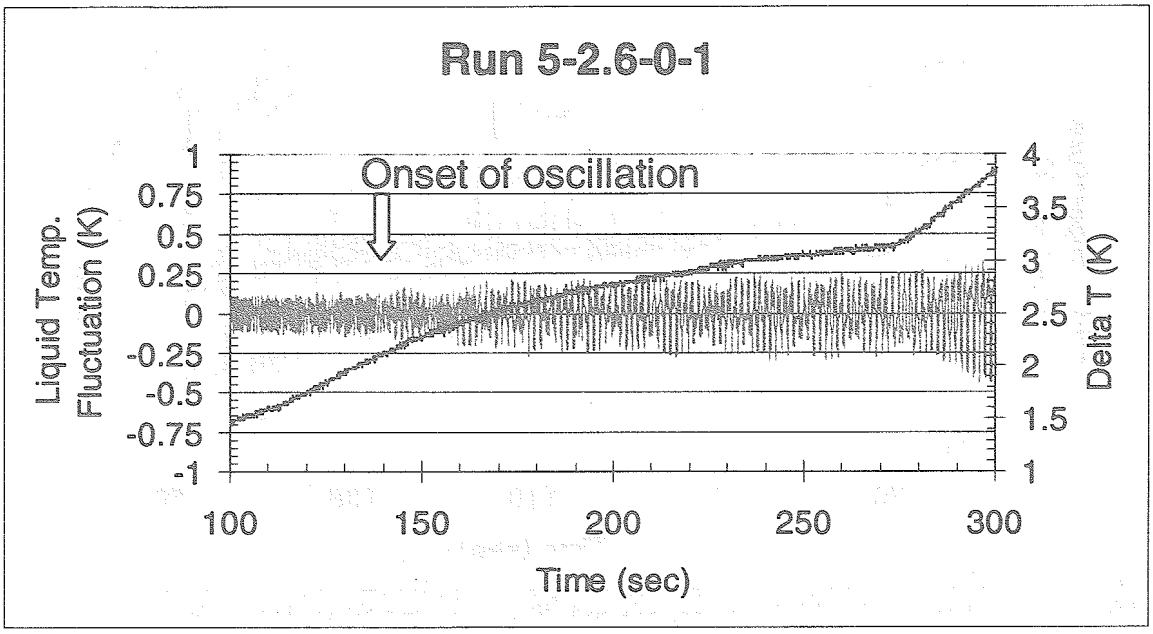


Figure 7.3 Methanol bridge temperature and disk temperature variation at the onset of oscillatory convection for D = 5.0 mm, H = 2.6 mm, AR = 1.04

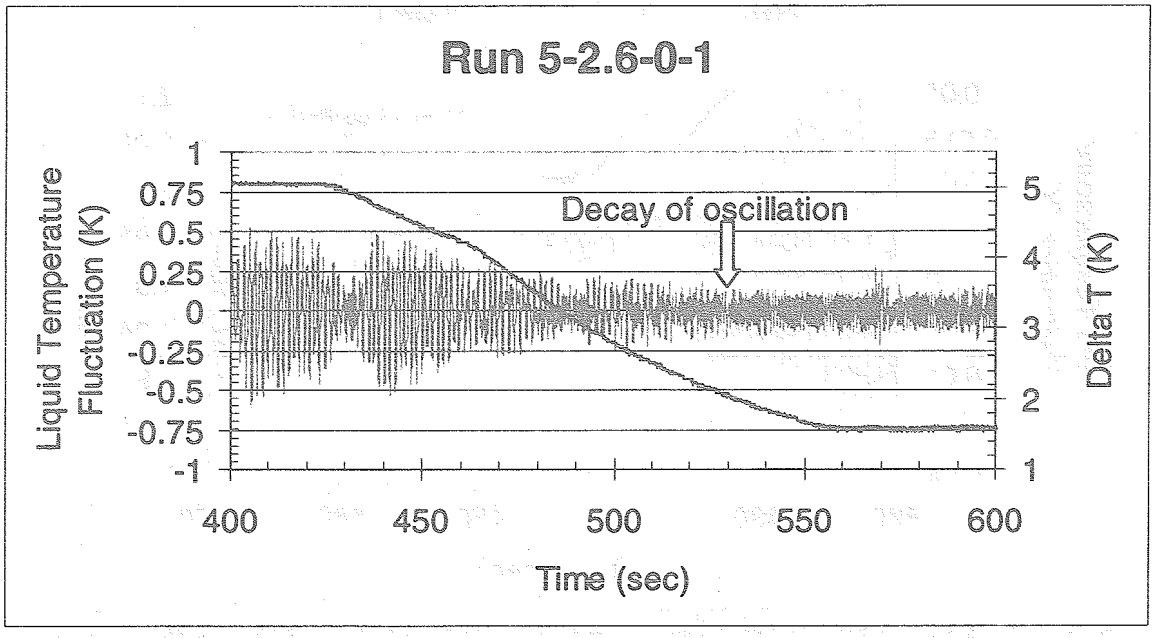


Figure 7.4 Methanol bridge temperature and disk temperature variation at the end of oscillatory convection for D = 10.0 mm, H = 2.6 mm, AR = 1.04

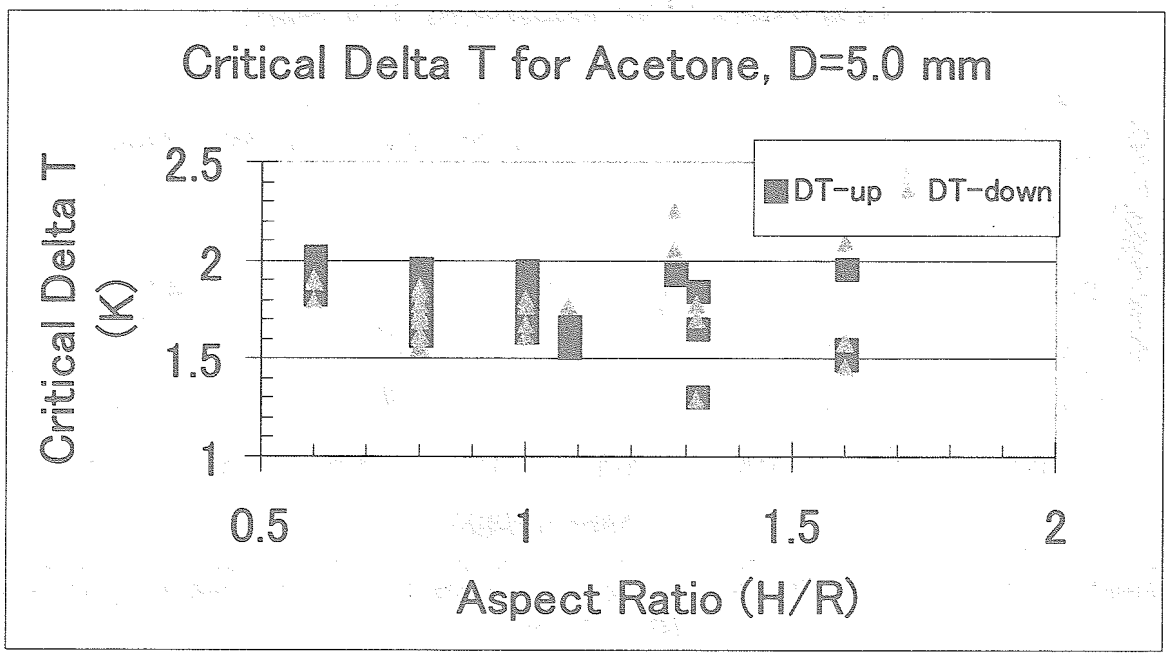


Figure 7.5 Variation of critical disk temperature difference with aspect ratio for acetone (D= 5.0mm)

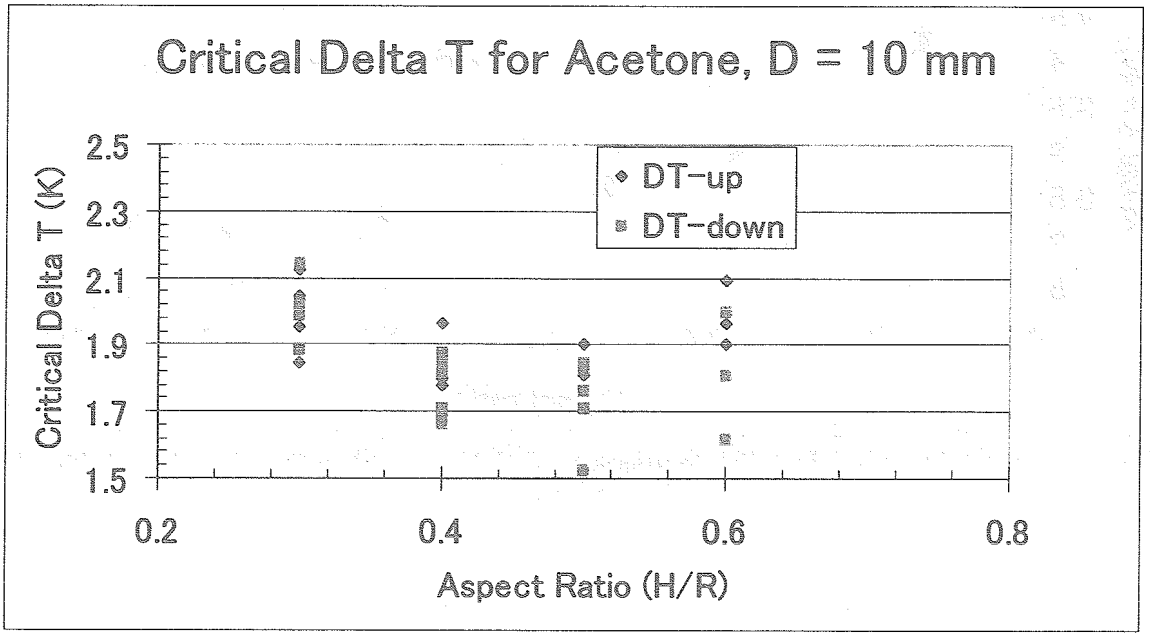


Figure 7.6 Variation of critical disk temperature difference with aspect ratio for acetone (D= 10.0 mm)

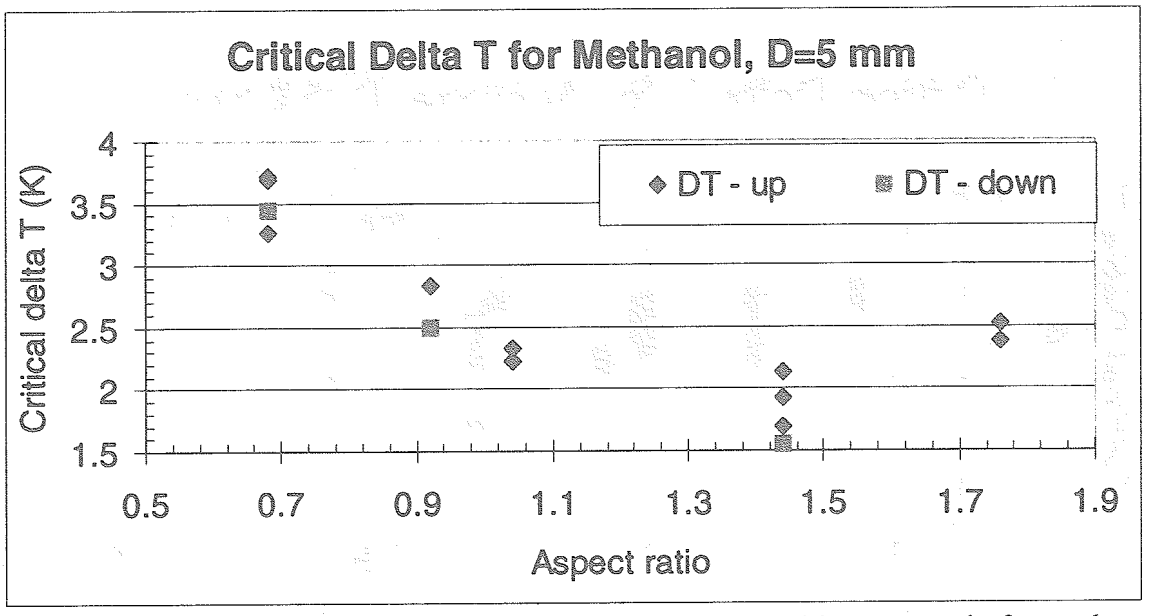


Figure 7.7 Variation of critical disk temperature difference with aspect ratio for methanol (D= 5.0 mm)

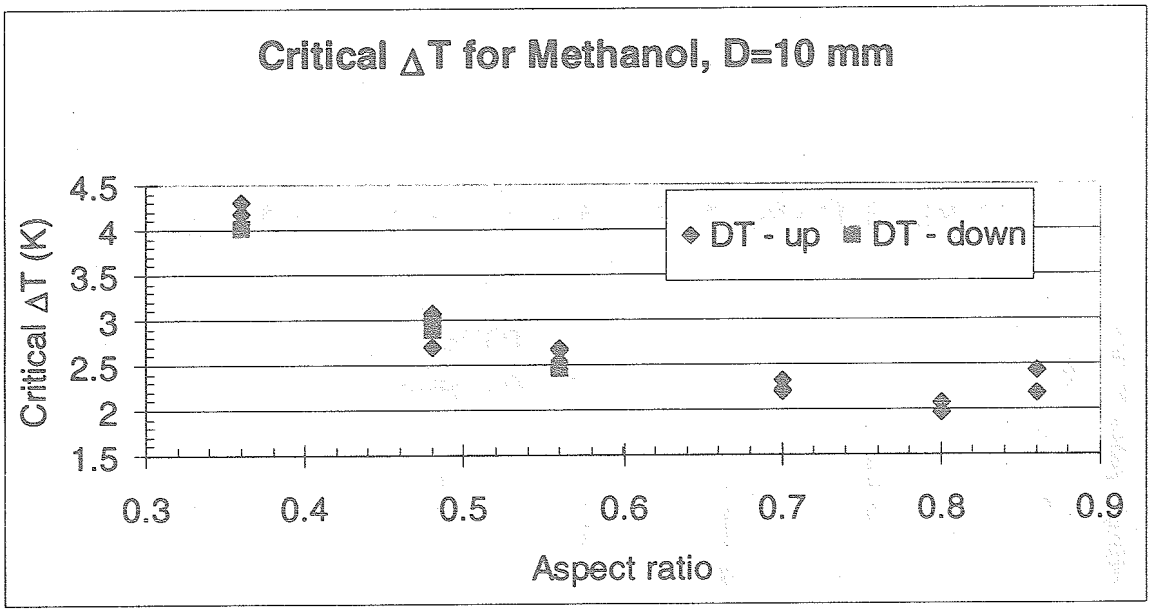


Fig. 7.8 Variation of critical disk temperature difference with aspect ratio for methanol (D=10.0 mm)

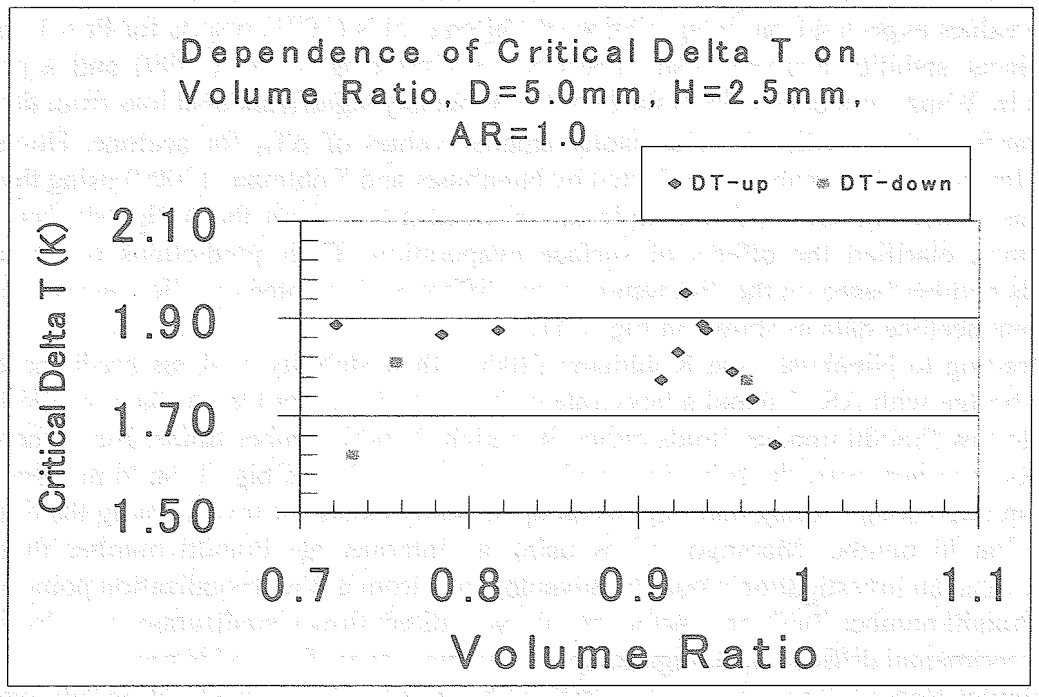


Fig. 7.9 Variation of $\Delta T_{cr}$ with volume ratio for acetone
(D= 5.0 mm, H= 2.5 mm, AR = 1.0)

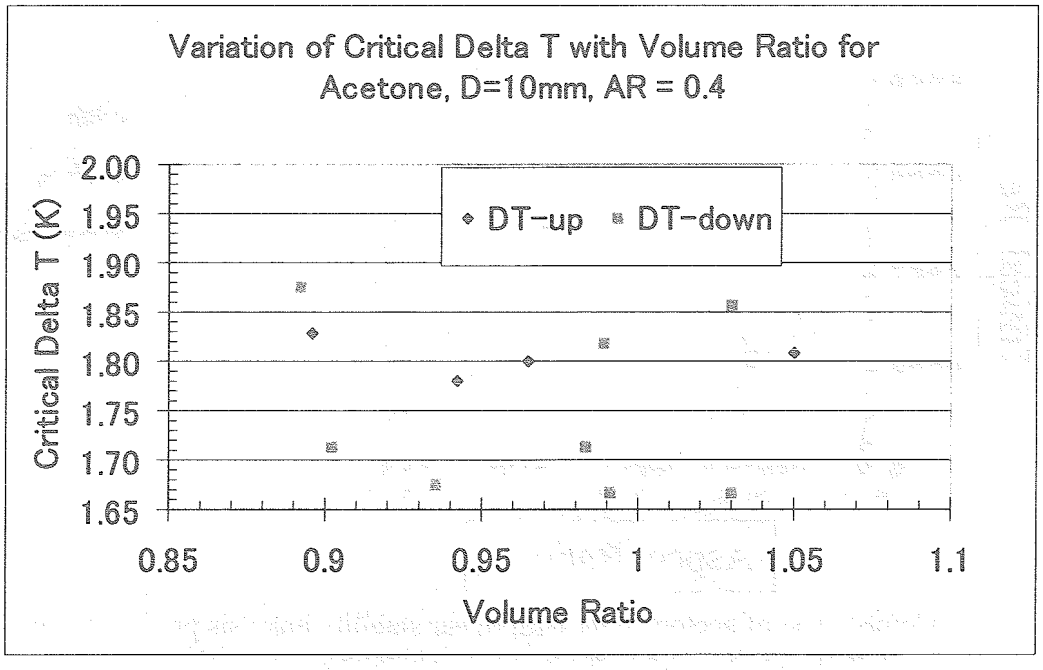


Fig. 7.10 Variation of $\Delta T_{cr}$ with volume ratio for acetone
(D= 10.0mm, H= 2.0 mm, AR = 0.4)

### 7.2 Comparison with Linear Stability Analysis Results for Acetone

The critical disk temperature difference data for acetone will be later shown to be higher than the values expected from interpolation of Velten et al.'s (1991) results for Pr = 1 and 7. A recent linear stability analysis result reported by Kuhlmann et al. (1999) and a previous analysis by Wanschura et al. (1997) for Pr = 4 without any significant heat loss from the liquid bridge surface also predicted significantly smaller values of $\Delta T_{cr}$ for acetone. However, a recent a linear stability analysis conducted by Nienhuser and Kuhlmann (2000) using the actual properties of acetone and with a simple model of heat loss from the bridge surface due to evaporation, clarified the effects of surface evaporation. Their predictions of the critical Reynolds number based on the disk temperature difference indicated excellent agreement with the present acetone data as shown in Fig. 7.11.

According to Nienhuser and Kuhlmann (2000), their stability analysis predicted that an acetone bridge with AR=1.0 and a large rate of heat loss from the free surface, would behave similar to low Prandtl number fluids rather than high Prandtl number fluids. But if there were no evaporation heat loss, the behavior would be similar to that of high Prandtl number fluids. This is an interesting finding that implies an opportunity exists for investigating the dynamics of low Prandtl number Marangoni flow using an intermediate Prandtl number fluids like acetone. Such an investigation would be advantageous from a flow visualization point of view, as low Prandtl number fluids are opaque and prevent direct flow visualization, and also present other experimental difficulties at high temperatures such as surface oxidation.

A similar stability analysis for methanol with a much smaller evaporation rate would be expected to yield results that would match the experimental values without taking into account the evaporation effects.

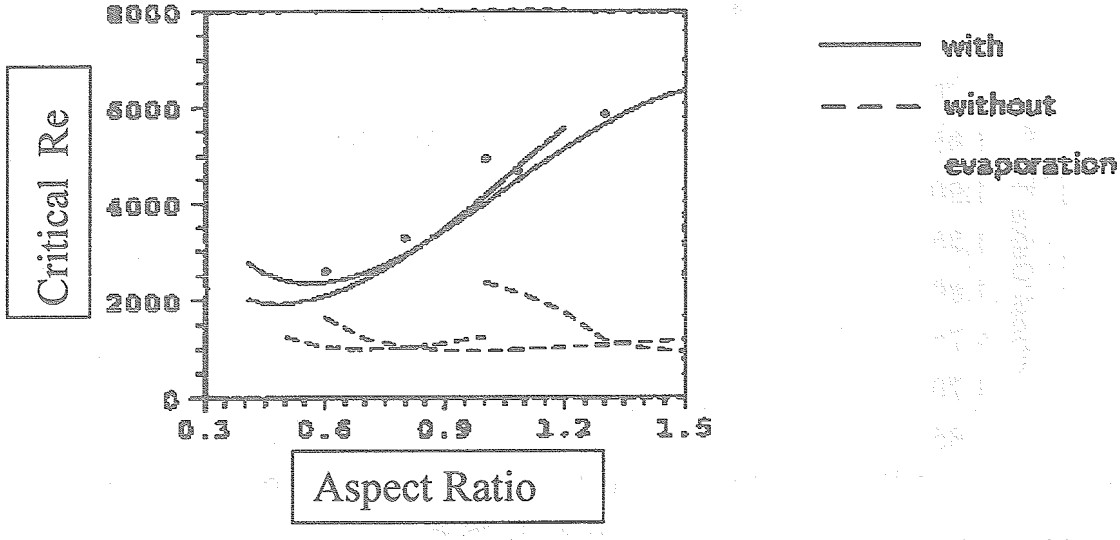


Figure 7.11 Comparison of acetone data with linear stability analysis predictions with and without surface evaporation (from Nienhuser et al., 2000)

### 7.3 Critical Marangoni Number

Based on the critical temperature differences measured, the critical Marangoni Number, $Ma_{cr}$, was calculated using two different definitions used in previous studies:

$$Ma_R2_{/H} = (|\partial\sigma/\partial T|\Delta T_{cr} R^2) / \mu\alpha H \qquad (1)$$

$$Ma_H = (|\partial\sigma/\partial T|\Delta T_{cr} H) / \mu\alpha \qquad (2)$$

where H is the liquid bridge height, R is the bridge radius, $\mu$ is dynamic viscosity and $\alpha$ is thermal diffusivity. Velten et al. (1991) used the first definition, while many other authors have used the second definition.

The critical Marangoni number data based on the onset of liquid temperature fluctuations for a volume ratio of about 100% are plotted against the aspect ratio, H/R, for different disk diameters in Figs. 7.12 and 7.13 for acetone and in Figs. 7.14 and 7.15 for methanol. Both of the critical Marangoni numbers, $Ma_R2_{/H}$ and $Ma_H$, are seen to increase with the disk diameter. While $Ma_R2_{/H}$ decreased with the aspect ratio as in Velten et al.'s (1991) results, $Ma_H$ increased with the aspect ratio as reported previously by Vargas (1982) for a higher Prandtl number fluid.

As mentioned earlier and now shown in Fig. 7.16, the critical Marangoni ($Ma_R2_{/H}$) numbers for D = 5 mm were found to be significantly higher than the values interpolated from Velten et al.'s (1991) data for Pr = 1 and 7 obtained for a disk diameter of 6 mm. Although the reasons for this difference are not perfectly clear, a significant difference between acetone and molten salts (KCl and $NaNO_3$) used by Velten et al. (1991) is the difference in the rate of heat loss from the liquid bridge surface. Although molten salt bridges must have had some heat loss from the bridge surface due to radiation heat transfer, its magnitude is considered to be much less than that of acetone due to a high rate of surface evaporation, because of the latent heat involved in phase change. Surface evaporation can be regarded as a significant heat sink in the system in addition to the cold disk. This extra heat loss from the free surface due to evaporation may have necessitated a greater temperature difference to be applied to cause oscillatory convection than otherwise needed without any evaporation.

In contrast, the critical Marangoni numbers for methanol agreed well with Velten et al.'s data for Pr = 7. Since the evaporation rate for methanol was found to be ¼ to 1/5 of that of acetone, the evaporation effects are considered to be less significant and it is reasonable that the difference in the critical Marangoni number data between methanol data and Velten et al.'s data is essentially eliminated.

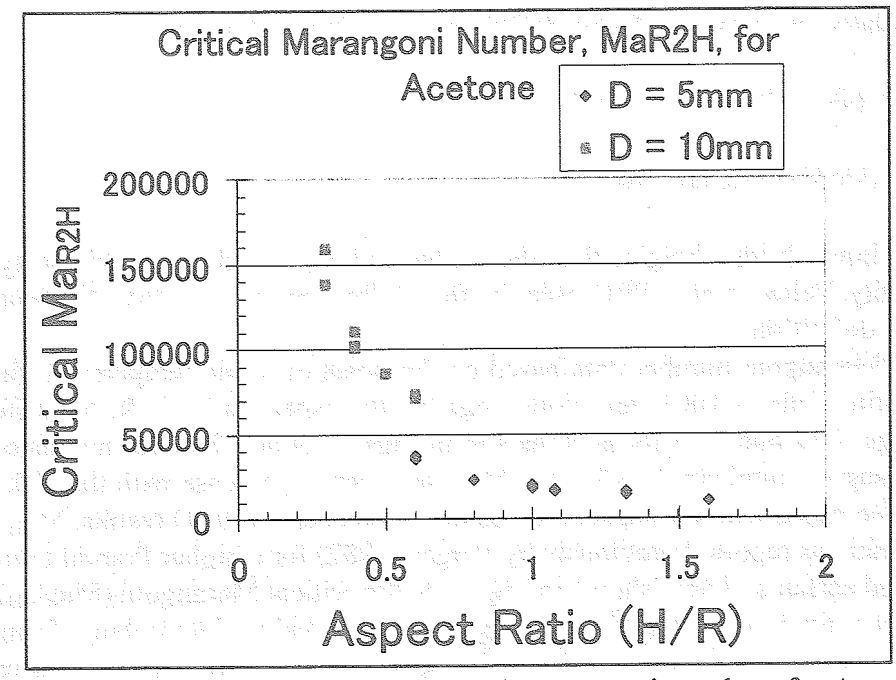


Figure 7.12 Comparison of critical Marangoni numbers for Acetone between D = 5.0 mm and 10.0 mm

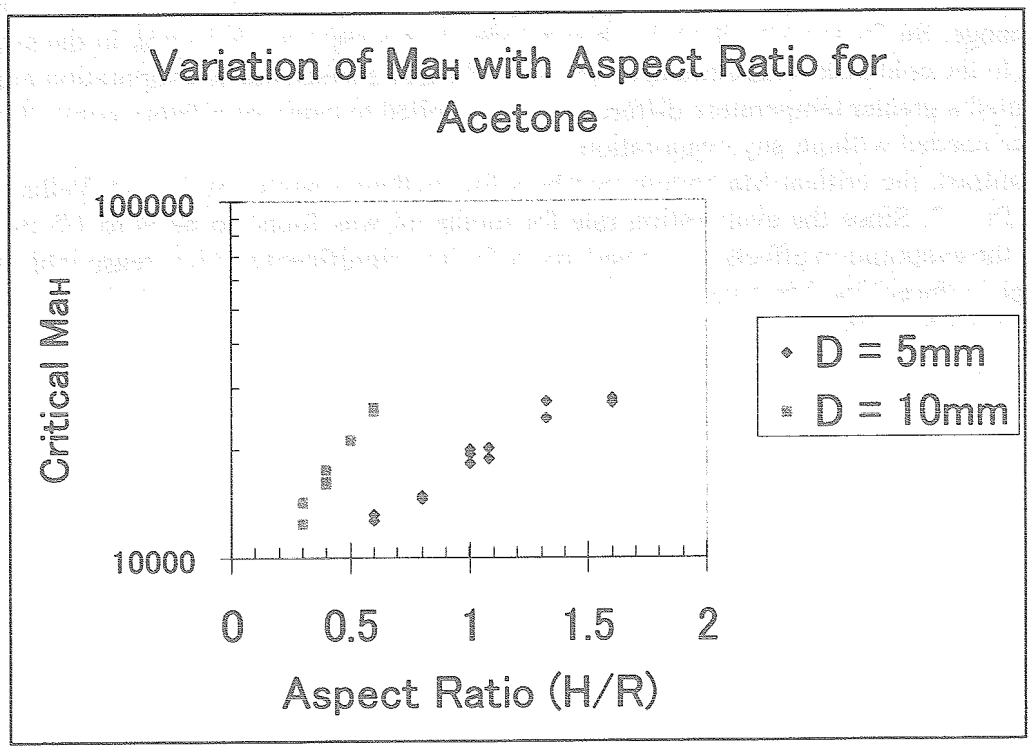


Figure 7.13 Variation of critical Marangoni number, $Ma_H$, with aspect ratio for acetone

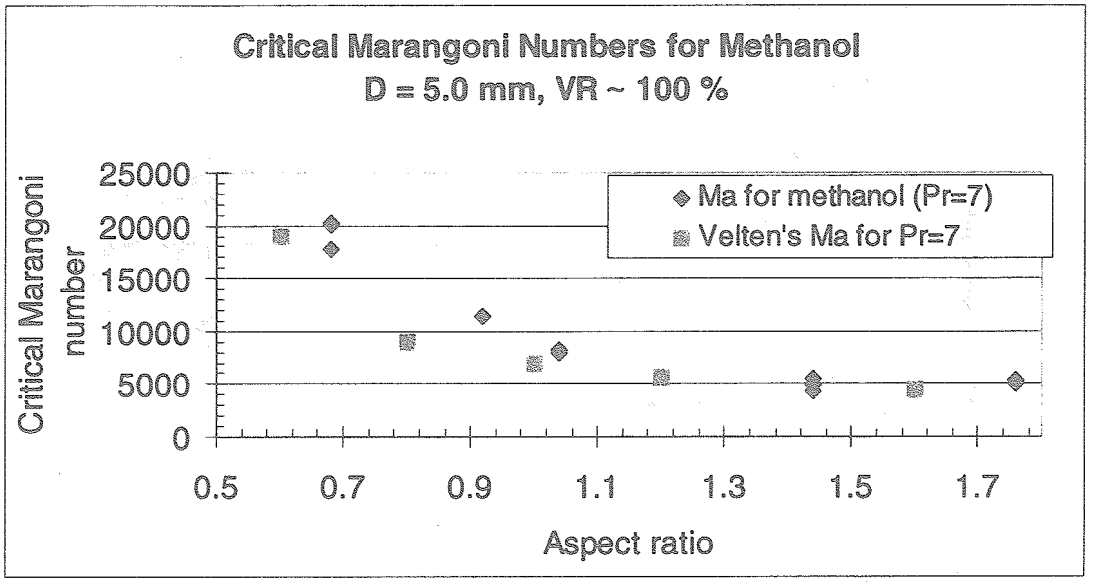


Figure 7.14 Variation of critical Marangoni number, $Ma_{R2/H}$, with aspect ratio for methanol (D = 5.0 mm)

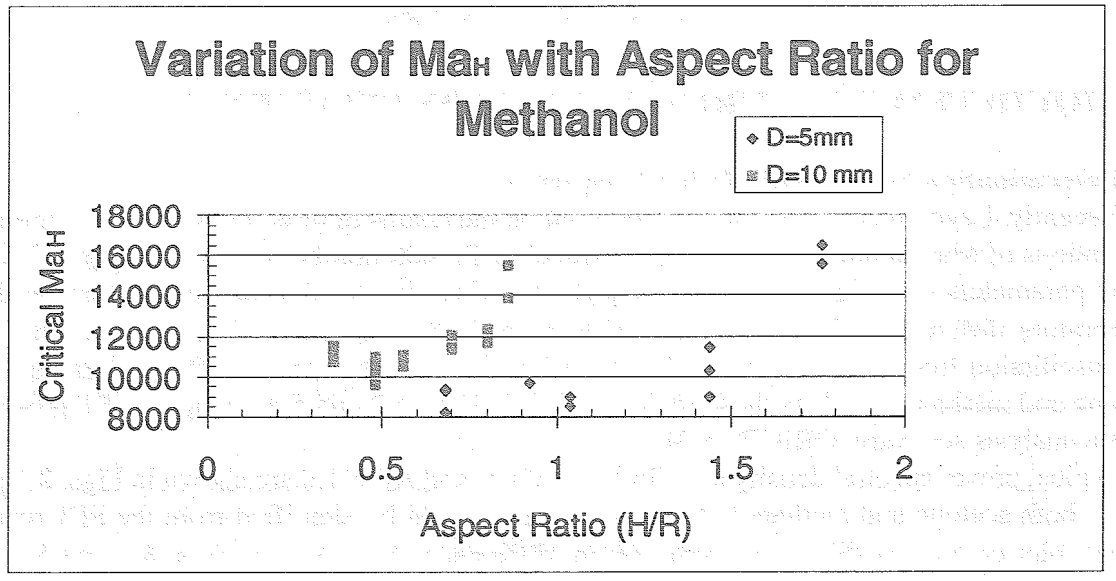


Figure 7.15 Variation of critical Marangoni number, $Ma_H$, with aspect ratio for methanol

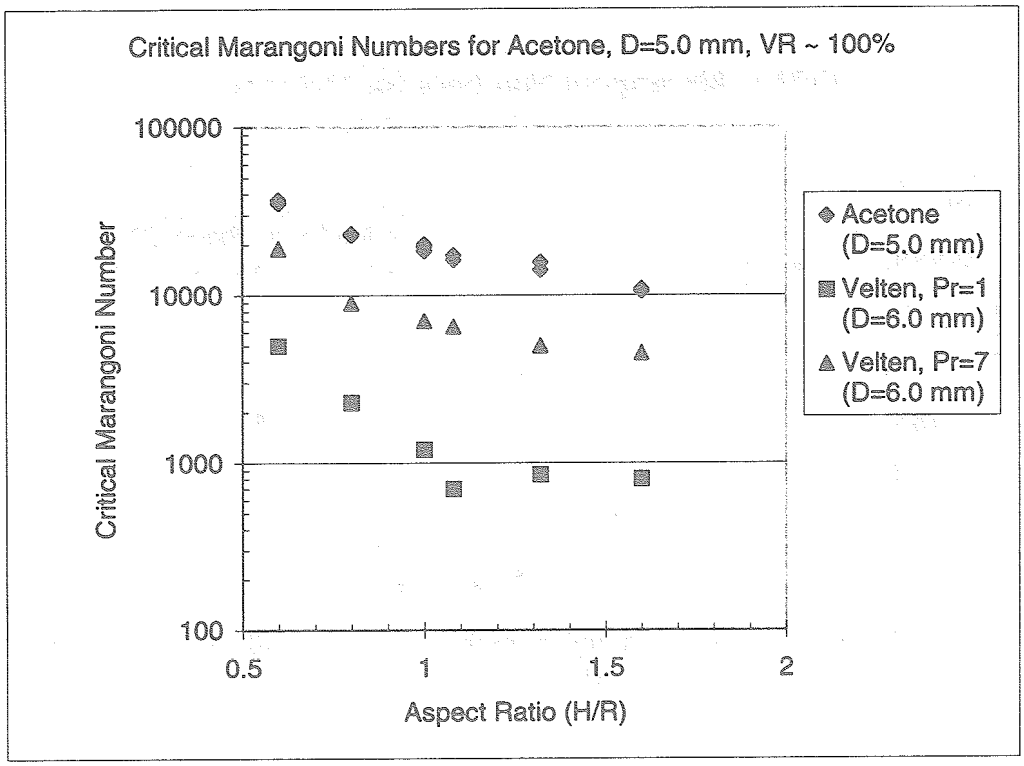


Figure 7.16 Comparison of critical Marangoni numbers, $Ma_{R2/H}$, for acetone with Velten et al.'s (1991) data

# 8. LIQUID TEMPERATURE OSCILLATION FREQUENCY

## 8.1 Determination of Peak Oscillation Frequency

Recently, Leypold et al. (2000) have reported on the results of three-dimensional numerical simulations of Marangoni convection in intermediate Prandtl number fluids, Pr = 4 and 7. One of the parameters investigated was the frequency of flow and temperature oscillations at disk temperature differences above $\Delta T_{cr}$. In order to verify the numerical simulation results, the peak oscillation frequency data were obtained from the liquid temperature fluctuation data for acetone and methanol, such as those shown earlier in Figs. 5.2 and 5.4, using an FFT program in data analysis software, ORIGIN 5.0J.

Typical power spectral density data for D = 5.0mm and AR = 1.0 are shown in Figs. 8.1 and 8.2 for both acetone and methanol. A peak frequency could be identified from the FFT results and are plotted against the excess temperature difference, $\Delta T - \Delta T_{cr}$ in Figs. 8.3 and 8.4 for acetone and methanol, respectively. Both of these graphs show linear variations with the excess temperature difference, however, the slopes are significantly different between acetone and methanol.

## 8.2 Comparison of Data with Numerical Simulation Results

Leypold et al. (2000) also predicted a linear increase in the non-dimensional oscillation frequency with the increase in Reynolds number (=Ma/Pr), which is based on $\Delta T$ as follows.

$$\omega = 28.9 + 7.0\,(Re - Re_c)/Re_c \qquad (3)$$

Thus, the numerical simulation result for Pr = 4 and AR = 1.0 is consistent with both the acetone and methanol data shown in Figs. 8.3 and 8.4.

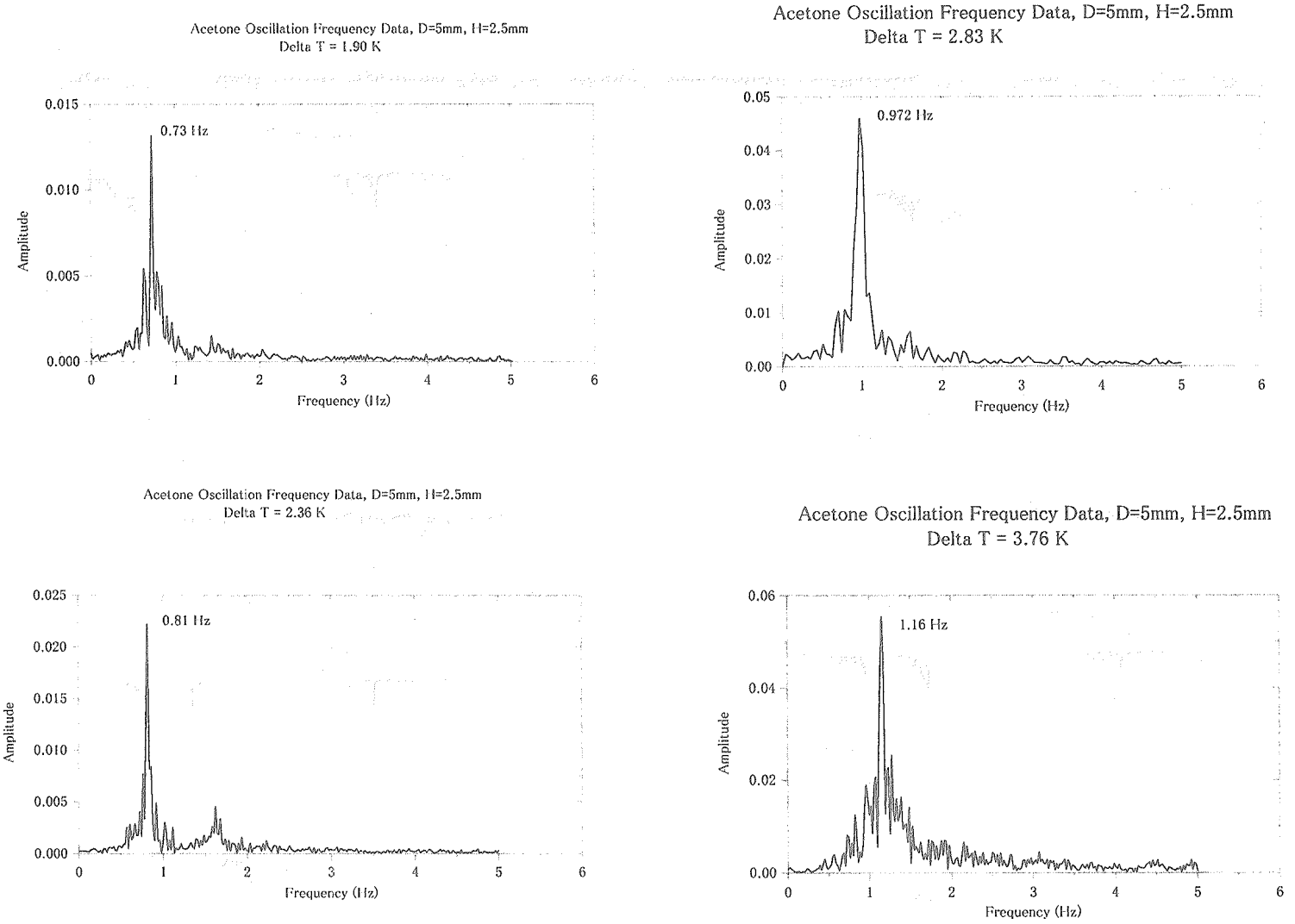


Figure 8.1 Typical power spectrum data for acetone temperature oscillations, D = 5.0 mm, H = 2.5 mm, AR = 1.0

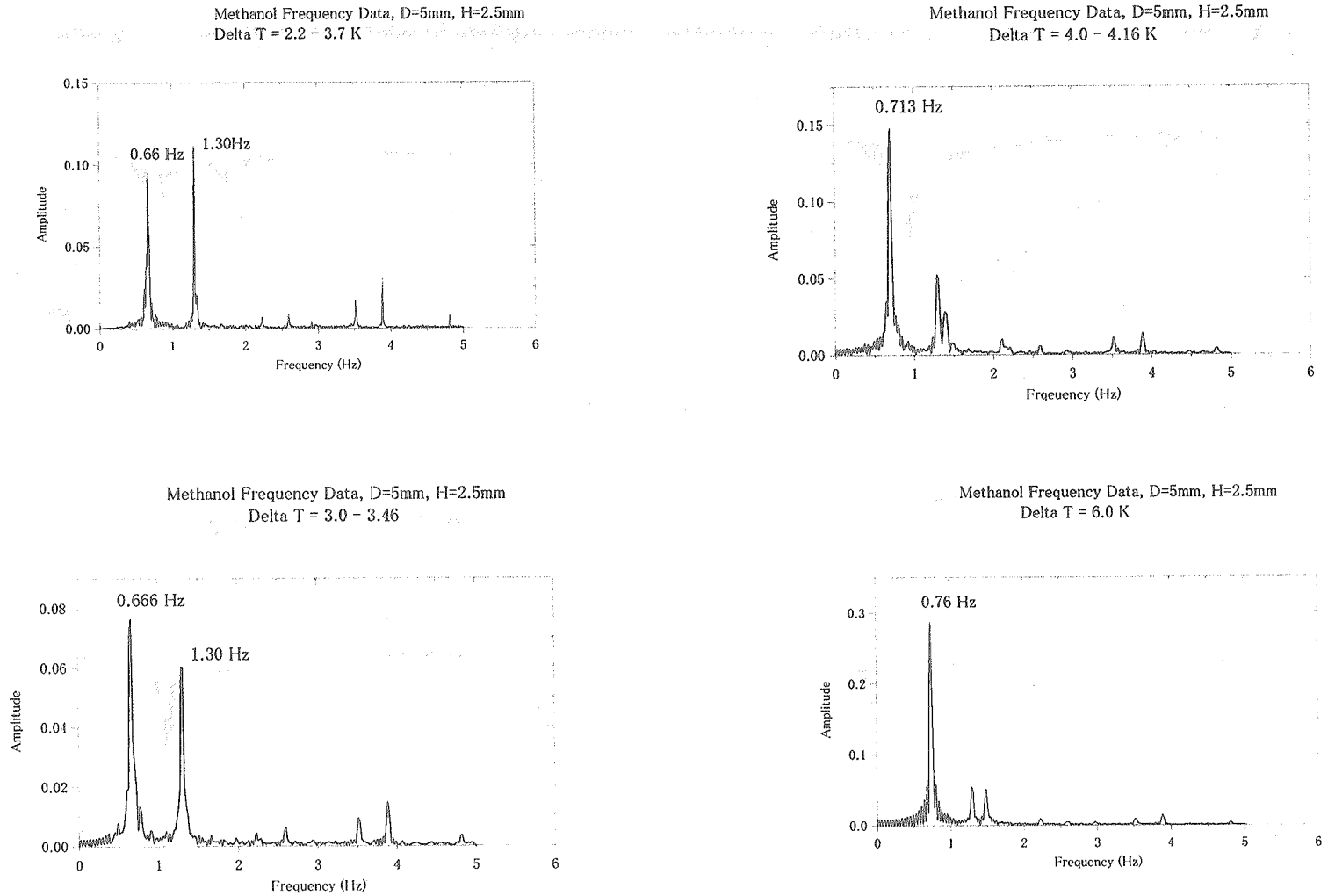


Figure 8.2 Typical power spectrum data for methanol temperature oscillations, D = 5.0mm, H=2.5mm, AR=1.0

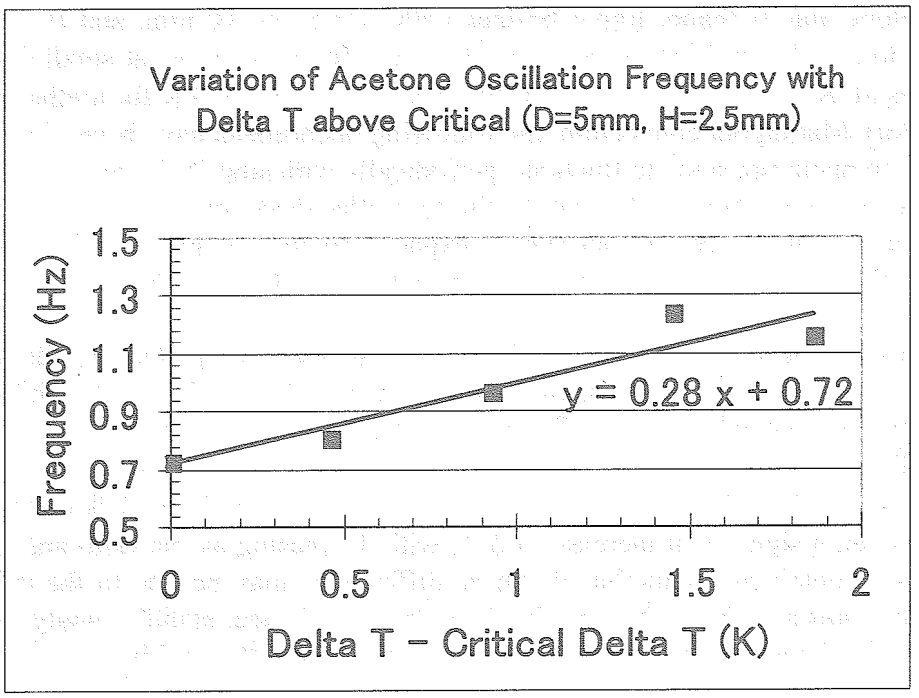


Figure 8.3 Variation of acetone temperature oscillation frequency with disk temperature difference, D= 5.0 mm, H= 2.5mm, AR = 1.0

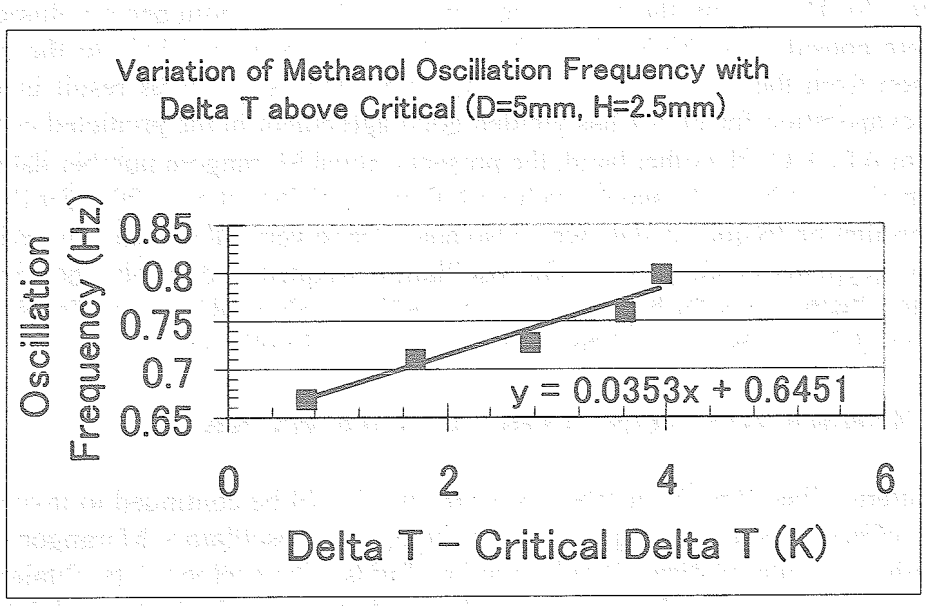


Figure 8.4 Variation of methanol temperature oscillation frequency with disk temperature difference, D= 5.0mm, H= 2.5mm, AR = 1.0

## 9. SUMMARY OF EXPERIMENTAL RESULTS

In acetone and methanol liquid bridges with D = 5 and 10 mm, and H = 1.5 ~ 4.5 mm, transition to oscillatory Marangoni convection was found to occur at small disk temperature differences of $\Delta T_{cr}$ = 1.6 ~2.3 K for acetone, and $\Delta T_{cr}$ = 1.6 ~ 4.3 K for methanol. At the onset of oscillatory Marangoni convection, the following phenomena have been observed to occur:

1) liquid temperature starts to fluctuate periodically with amplitudes as small as 0.02 ~ 0.1 K,
2) surface velocity starts to fluctuate in the azimuthal direction,
3) vortices below the free surface start to expand and contract periodically, and
4) radial flow patterns near the mid-plane start to oscillate or rotate.

On the other hand, the surface oscillations and temperature pattern oscillations just below the upper disk could not be detected clearly, possibly due to the small critical temperature differences involved which are sufficient to cause oscillatory convection but insufficient to cause surface oscillations.

The critical $\Delta T$ values for acetone did not vary strongly with the disk diameter and aspect ratio, however, a significant increase in $\Delta T_{cr}$ with decreasing aspect ratio and increasing disk diameter was obtained for methanol. These differences may be due to the difference in the evaporation rates and their effect on the flow behavior. Linear stability analyses have pointed out a possible change in the flow behavior of acetone from that of high Prandtl number fluids without any evaporation to low Prandtl number fluids with evaporation.

The critical Marangoni number data for both acetone and methanol varied strongly with the disk diameter and aspect ratio, as has been previously observed for higher Prandtl number fluids. Compared to the critical Marangoni numbers for Pr ≈ 4 interpolated from Velten et al.'s (1991) data for D = 6 mm, the present acetone data for D = 5 mm and a volume ratio close to 100% were considerably higher by a factor of 2 ~ 3, due most likely to the effect of liquid evaporation from the free surface. A recent linear stability analysis result incorporating the effect of evaporation for Pr = 4 has yielded good agreement in the predicted critical Reynolds number (or $\Delta T_{cr}$ ). On the other hand, the present critical Marangoni number data for much less volatile methanol (Pr = 6.8) agreed well with those of Velten et al. (1991) for Pr = 7.

The oscillation frequency data were also analyzed to verify the recent numerical simulation results of Leypolds et al. (2000). The oscillation frequency data obtained from the liquid temperature fluctuations for both acetone and methanol showed linear variations with the disk temperature differences, as predicted by the numerical simulation.

## 10.RECOMMENDATIONS FOR FUTURE WORK

The intermediate Prandtl number experiments should be continued to investigate in more detail the effects of surface evaporation on the onset of oscillatory Marangoni convection in liquid bridges of intermediate Prandtl number fluids. The acetone data obtained so far have been successfully used to check some of the predictions of the linear stability analysis and numerical simulations.

Based on the successful prediction of the acetone data by the linear stability analysis with a simple evaporation model, the evaporation rate should be better quantified so that a more rigorous model of surface evaporation can be developed and incorporated into both the linear stability analysis and numerical simulation models. The dependence of surface evaporation rate on the liquid temperature, surrounding temperature and pressure, partial pressure and latent heat should be further investigated for both acetone and methanol.

Internal temperature distributions in acetone bridges under steady and oscillatory

convection should also be determined using a thermocouple mounted on a traversing stage so that the thermocouple junction can be positioned precisely in different parts of the liquid bridge. An infrared imager should also be used to measure the temperature distributions on the free surface by fabricating an enclosure using a zinc-selenide plate to transmit infrared wavelengths. These results can then be compared with the linear stability analysis and numerical simulation results to verify the hypothesis that strong surface evaporation for an intermediate Prandtl number fluid changes the Marangoni convection characteristics similar to those of low Prandtl number fluids.

**ACKNOWLEDGEMENTS:** Authors gratefully acknowledge National Space Development Agency of Japan (NASDA) for this work. Administrative support from Mr. T. Arai and Dr. K. Takagi of NASDA Space Utilization Research Center is also gratefully acknowledged.

## REFERENCES

Chen, Q.S. and Hu, W.R.: "Influence of liquid bridge volume on instability of floating half zone convection", Int. J. Heat Mass Transfer, Vol. 41, Nos. 6-7 (1998), pp.825-837.

Chun, Ch.-H. and Wuest, W.: "Experiments on the transition from the steady to the oscillatory Marangoni-convection of a floating zone under reduced gravity effect," Acta Astronautica, Vol. 6 (1979), pp.1073-1082.

Hibiya, T., Nakamura, S., Azami, T., Sumiji, M., Imaishi, N., Mukai, K., Onuma, K. and Yoda, S.: "Marangoni flow of molten silicon", IAF-99-IAA.12.1.03, a paper presented at the 50th Int. Astronautical Congress, Oct. 4-8, 1999, Amsterdam, The Netherlands.

Hirata, A., Nishizawa, S. and Sakurai, M.: "Experimental Results of Oscillatory Marangoni convection in a liquid bridge under normal gravity", J. of Japan Soc. Microgravity Applications, Vol. 14, No.2 (1997), pp. 122-129.

Kamotani Y., Ostrach, S. and Vargas, M.: "Oscillatory thermocapillary convection in a simulated float-zone configuration", J. Crystal Growth, Vol. 66(1984), pp. 83- 90.

Kawaji, M., Ahmad, W., DeJesus, J.M., Sutharsan,B., Lorencez, C. and Ojha, M.: "Flow Visualization of Two-Phase Flows using Photochromic Dye Activation Method", Nuclear Engineering and Design, Vol.141(1993), pp. 343-355.

Kawaji, M.: "Two-phase flow measurements using a photochromic dye activation technique," Nuclear Engineering and Design, Vol. 184(1998), pp.379-392.

Kitagawa, T., Nishino, K. and Yoda, S.: "Temperature oscillation and dynamic surface deformation for the onset of oscillatory flow in a liquid column", J. Japan Soc. of Microgravity Application, Vol. 16, Supplement(1999), pp. 100-101.

Kuhlmann, H.C. and Rath, H.J.: "On the interpretation of phase measurements of oscillatory thermocapillary convection in liquid bridges," Phys. Fluids A, Vol. 5(1993), pp.2117-2120.

Leypold, J., Kuhlmann, H.C. and Rath, H.J.: "Three-dimensional numerical simulation of thermocapillary flows in cylindrical liquid bridges", accepted for publication in J. Fluid Mechanics (2000).

Nienhuser, Ch. And Kuhlmann, H.C.: "Floating zone stability I. Cylinder: Medium Prandtl numbers, II. Deformed surfaces", presented at the NASDA Meeting on Marangoni convection research, Tokyo, March 6, 2000.

Onuma, K., Sumiji, M., Nakamura, S. and Hibiya, T.: "Direct observation of Marangoni convection-induced oscillation at silicon melt surface," Applied Physics Letters, Vol. 74, No. 23(1999), pp.3570-3572.

Otsubo, F., Kuwahara, L., Doi, T. and Yoda, S.: "The visualization experiment on the temperature oscillations and convective behavior of Marangoni convection in the liquid bridge", J. Japan Soc. of Microgravity Application, Vol. 16, Supplement(1999), pp. 98-99.

Preisser, F., Schwabe, D. And Scharmann, A.: "Steady and oscillatory thermocapillary convection in liquid columns with free cylindrical surface", J. Fluid Mechanics, Vol. 126(1983), pp. 545-567.

Tudose, E.T. and Kawaji, M.: "An experimental study of thermocapillary convection in a thin horizontal liquid layer in a rectangular cavity under normal gravity with and without controlled vibration", IAF-99-J.4.08, a paper presented at the 50th Int. Astronautical Congress, Oct. 4-8, 1999, Amsterdam, The Netherlands.

Tudose, E.T. and Kawaji, M.: "An experimental investigation of the onset of oscillations in thermocapillary-buoyant flows in a rectangular cavity", a paper accepted for presentation at the 34th National Heat Transfer Conference, August 20-22, 2000, Pittsburgh, Pennsylvania.

Vargas, M.: "Oscillatory thermocapillary flow in a simulated floating-zone configuration," M.Sc. thesis, Case Western Reserve University, 1982.

Velten, R., Schwabe, D. And Scharmann, A.: "The periodic instability of thermocapillary convection in cylindrical liquid bridges", Phys. of Fluids, A., Vol. 3, No. 2(1991), pp. 267-279.

Wanschura, M., Kuhlmann, H.C., and Rath, H.J.: "Linear stability of two-dimensional combined buoyant-thermocapillary flow in cylindrical liquid bridges", Physical Review E, Vol. 55(6), (1997) 7036-7042.

Yao, Y.L., Liu, F. and Hu, W.R.: "How to determine critical Marangoni number in half floating zone convection," Int. J. Heat and Mass Transfer, Vol.39, No.12(1996), p.2539.